



Integrated Multi-omics, Virtual Screening and Molecular Docking Analysis of Methicillin-Resistant *Staphylococcus aureus* USA300 for the Identification of Potential Therapeutic Targets: An In-Silico Approach

Shakilur Rahman¹ · Amit Kumar Das¹

Accepted: 10 September 2021 / Published online: 17 September 2021
© The Author(s), under exclusive licence to Springer Nature B.V. 2021

Abstract

Staphylococcus aureus infection is a leading cause of mortality and morbidity in community, hospital and live-stock sectors, especially with the widespread emergence of methicillin-resistant *S. aureus* (MRSA) strains. To identify new drug molecules to treat MRSA patients, we have undertaken to search essential proteins that are indispensable for their survival but non-homologous to human host proteins. The current study utilizes a subtractive genome and proteome approach to screen the possible therapeutic targets against *S. aureus* USA300. Bacterial essential genes are obtained from the DEG database and are compared to avoid cross-reactivity with human host genes. In silico analysis shows 198 proteins that may be considered as therapeutic candidates. Depending on their sub-cellular localization, proteins are grouped as either vaccine or drug targets or both. Extracellular proteins such as cell division proteins (Q2FZ91, Q2FZ95), penicillin-binding proteins (Q2FZ94, Q2FY10) of the bacterial cell wall, phosphoglucomutase (Q2FE11) and lipoteichoic acid synthase (Q2FIS2) are considered as vaccine targets, and their epitopes have been mapped. Altogether, 53 drug targets are identified, which have shown similarity with the drug targets available in the DrugBank database. Predicted drug targets belong to the common metabolic pathways of MRSA, such as fatty acid biosynthesis, folate biosynthesis, peptidoglycan biosynthesis, ribosome, etc. Protein–protein interaction analysis emphasizing peptidoglycan biosynthesis reveals the connection between penicillin-binding proteins, mur-family proteins and FemXAB proteins. In this study, staphylococcal FemA protein (POA0A5) is subjected to structure-based virtual screening for the drug repurposing approach. There are 20 residues missing in the crystal structure of FemA, and 12 of these residues are located at the catalytic site. The missing residues are modelled, and stereochemistry is checked. FDA approved drugs available in the DrugBank database have been used in virtual screening with FemA in search of potential repurposed molecules. This approach provides us with 10 drugs that may be used in the treatment of methicillin-resistant staphylococcal mediated diseases. AutoDock 4.2 is used for in silico screening and shows a comparable inhibition constant (Ki) for all 10 FDA-approved drugs towards FemA. Most of these drugs are used in the treatment of various cancers, migraines and leukaemia. Protein–drug interaction analysis shows that the drugs mostly interact with hydrophobic residues of FemA. Moreover, Tyr328 and Lys383 contribute largely to hydrogen bondings during interactions. All interacting amino acids that bind to the drugs are part of the active site cavity of FemA.

Keywords *Staphylococcus aureus* · Methicillin-resistance · USA300 · USA300_tch1516 · FemA protein · Repurposing drugs

Introduction

Staphylococcus aureus is a catalase-positive, facultative anaerobic bacterium responsible for causing a wide variety of pus-forming infections of the skin in humans (Carleton et al. 2004). *S. aureus* secretes a bunch of superantigens into blood called enterotoxins, thereby causing food poisoning,

✉ Amit Kumar Das
amitk@bt.iitkgp.ac.in

¹ Department of Biotechnology, Indian Institute of Technology Kharagpur, Kharagpur, West Bengal 721302, India

toxic shock syndrome, etc. (Lina et al. 2004; Diekema et al. 2001). *S. aureus* primarily colonizes in anterior nares of the nose, skins, guts and intestinal tracts (Kluytmans et al. 1997; Sibbald et al. 2006). Up to 30% of the human population is the relentless carrier of *S. aureus* in our society (Peacock et al. 2001). Pathogenicity islands of *S. aureus* express adhesin and coagulase that causes host blood clotting, thereby making the bacteria resistant to phagocytic killing (Ko et al. 2013). Besides, *S. aureus* also produces hyaluronidase and lipases that are actively involved in drug resistance (Ibberson et al. 2014; Cadieux et al. 2014).

Among the drug-resistant strains, Methicillin-resistant *Staphylococcus aureus* (MRSA) has been included in the global priority list of antibiotic-resistant bacteria by the World Health Organization (WHO), considering the high mortality and morbidity associated with invasive infections. MRSA became more threatening when it started showing resistance to multiple antibiotics, including penicillin, oxacillin, amoxicillin, quinolones, macrolides, cephalosporins, tetracycline and chloramphenicol (Chopra and Roberts 2001; Weese and van Duijkeren 2010). Despite the diversity, ~70% of MRSA isolates belong to the major five sequence types (STs: ST22, ST8, ST5, ST239 and ST398) (Giulieri et al. 2020). Nowadays, half of the *S. aureus* strains have become methicillin-resistant. Methicillin-susceptible *S. aureus* (MSSA) acquired the methicillin-resistant gene *mecA* by a mobile genetic element staphylococcus cassette chromosome (SCC) during the horizontal gene transfer and gave rise to the MRSA (Ito et al. 1999). The SCC element carries the *mecA* designated as SCCmec, integrated into the chromosome of MRSA strains (Ito et al. 2001), and thirteen variants of SCCmec can be found to date (Kaya et al. 2018). It was immediately discovered that methicillin resistance is different from penicillin resistance in the MRSA phenotype as it does not involve direct inactivation of the antibiotics. Instead, the alternative penicillin-binding protein (PBP2a), a membrane-associated protein, interacts with β -lactam drugs and brings about resistance (Otero et al. 2013).

One of the Methicillin-resistant *Staphylococcus aureus* strains, USA300, first emerged in the late 1990s as a community-associated MRSA (CA-MRSA) in the USA (Diekema et al. 2014). USA300 evolved from a less virulent and less resistant ancestor circulating in Central Europe around 160 years ago (Strauß et al. 2017). Over time, it became a significant cause of skin and soft-tissue infections and added an overall burden to the MRSA disease (Talan et al. 2011; Moran et al. 2006). Also, for its virulence, USA300 has emerged as a major cause of healthcare-associated (HA) infections (Jenkins et al. 2009). Recently an outbreak of MRSA USA300 among HIV patients has been observed in Japan (Ikeuchi et al. 2021). Classical USA300 clone belongs to ST8 type and is characterized by specific genetic features like possession of SCCmecIV, Pantone-Valentine leucocidin

(PVL) and the arginine catabolic mobile element (ACME) (Planet et al. 2013). Although pulse-field-gel-electrophoresis (PFGE) patterns initially defined USA300, *S. aureus* USA300 strain gave rise to several variants worldwide over the years (Laupland et al. 2008; Simor et al. 2010; Alvarez et al. 2006; Rajan et al. 2015; Takadama et al. 2020). USA300_TCH1516 represents the hypervirulent strain of USA300 lineage from the ST8 group of MRSA (Coe et al. 2019).

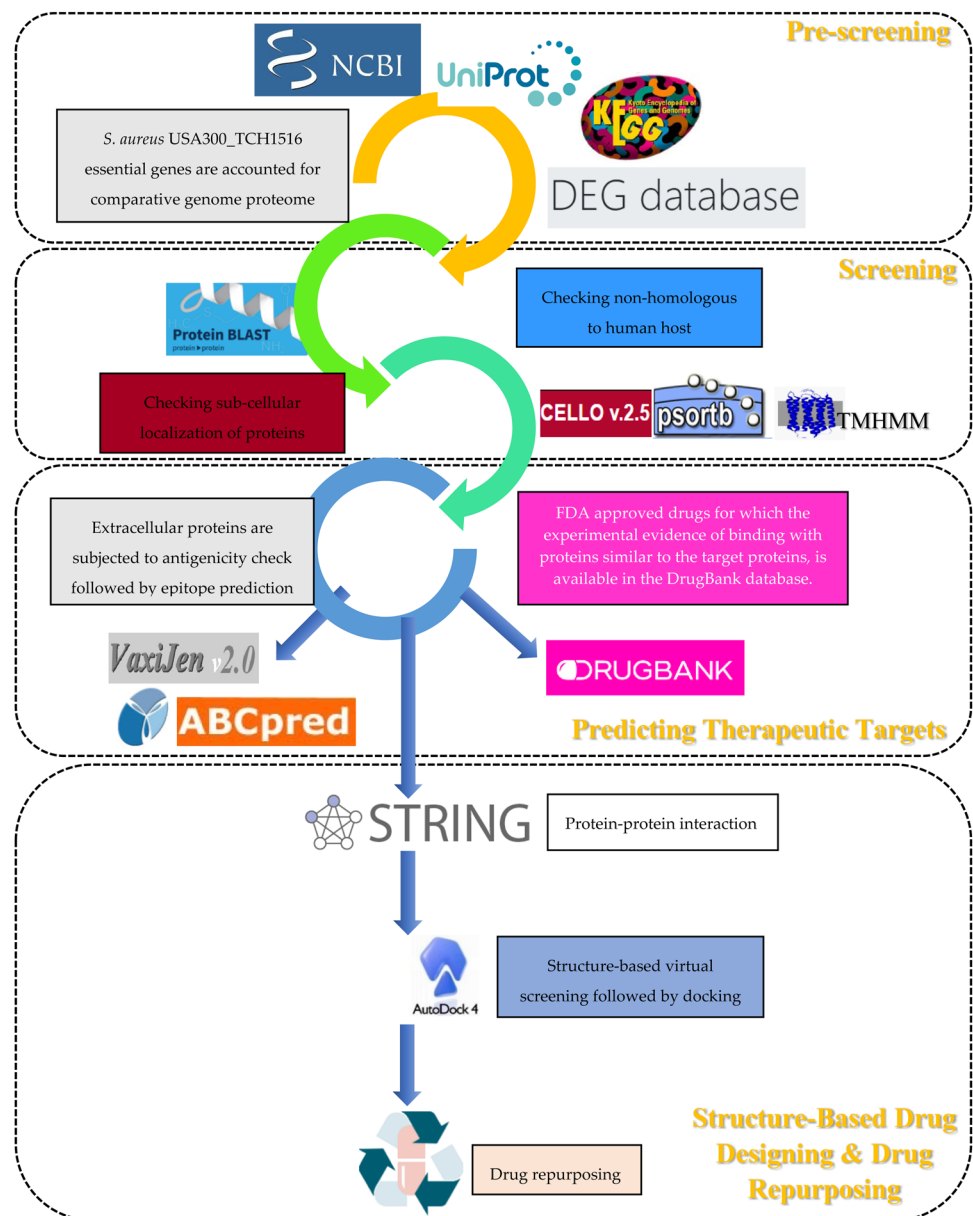
Methicillin-resistant *S. aureus* is a threat to humankind. Despite all the clinical significance, there is a lack of readily available vaccines in the market against the *S. aureus* bacteria. This bacterium expresses an extensive array of virulence factors such that a vaccine against any one of them may not be sufficient. Though there are many drugs available, but most of them are becoming ineffective with time. Hence it is required to find new drugs which may be used to treat infections caused by methicillin-resistant *S. aureus*. In this study, genomics and proteomics data of 14 virulent strains of *Staphylococcus aureus* have been used to understand their genetic features by an integrated interface for computational identification and visualization of genomic islands. Further, the metabolic pathway information of community-acquired methicillin-resistant *S. aureus* USA300_TCH1516 (KEGG organism: sax) strain is curated from Kyoto Encyclopaedia of Genes and Genomes (KEGG) in search of unique and common pathways between pathogen and host. Non-homologous essential proteins from the pathogen are screened against the DrugBank database for drug repurposing. These proteins have been docked with 1918 FDA-approved drugs obtained from the DrugBank database. This study presents the first approach to predict potential drug and vaccine targets for methicillin-resistant *S. aureus* USA300, applying the comprehensive subtractive genomics and proteomics computational approach (Fig. 1).

Materials and Methods

Evaluation of Genetic Diversity

Although *S. aureus* subsp. NCTC 8325 is the reference strain for the bacteria, but it may not represent the genetic features of every virulent strain. To understand the genetic features of all the *S. aureus* virulent strains, genomics and proteomics data of 14 virulent strains of *Staphylococcus aureus*; *S. aureus* RF122 (NC_007622), *S. aureus* subsp. aureus COL (NC_002951), *S. aureus* subsp. aureus JH1 (NC_009632), *S. aureus* subsp. aureus JH9 (NC_009487), *S. aureus* subsp. aureus MRSA252 (NC_002952), *S. aureus* subsp. aureus MSSA476 (NC_002953), *S. aureus* subsp. aureus Mu3 (NC_009782), *S. aureus* subsp. aureus Mu50 (NC_002758), *S. aureus*

Fig. 1 The schematic workflow of subtractive genome proteome analysis for predicting potential therapeutic targets for *Staphylococcus aureus* USA300. This study involves four steps, including Pre-screening, where genome, proteome data of *S. aureus* USA300_TCH1516 was retrieved from various databases followed by Screening. Bacterial essential proteins are checked for non-homologous to the human host, and sub-cellular localization analysis was performed in the Screening step. In the next step, B-cell epitopes were predicted for the extracellular proteins, and drug targets are identified from the pool of bacterial essential non-homologous proteins by searching in the DrugBank database for which the experimental evidence of binding with proteins similar to the target proteins are available. The final step involves the Structure-based drug designing and drug repurposing approach for an essential non-homologous protein selected based on protein-protein interaction analysis



subsp. *aureus* MW2 (NC_003923), *S. aureus* subsp. *aureus* N315 (NC_002745), *S. aureus* subsp. *aureus* NCTC 8325 (NC_007795), *S. aureus* subsp. *aureus* str. Newman (NC_009641), *S. aureus* subsp. *aureus* USA300_FPR3757 (NC_007793), and *S. aureus* subsp. *aureus* USA300_TCH1516 (NC_010079) were obtained by manual inspection from the virulence factor database (VFDB) (<http://www.mgc.ac.cn/VFs/main.htm>) (Liu et al. 2019). To understand the existence and positions of the virulent factors in these 14 genomes, the genomic visualization of these curated virulence factors was performed using IslandViewer 4: an integrated interface for computational identification and visualization of genomic islands (<http://www.pathogenomics.sfu.ca/islandviewer/>) (Bertelli et al. 2017). NCBI blastn (Johnson et al. 2008) was performed to

check the percentage of genomic similarity of the other 13 pathogenic strains with USA300_TCH1516 of *S. aureus*.

Identification of Metabolic Pathways

In search of unique and common pathways between pathogen and host, metabolic pathway information of community-acquired methicillin-resistant *S. aureus* USA300_TCH1516 (KEGG organism: sax) strain was curated from the Kyoto Encyclopedia of Genes and Genomes (KEGG; <https://www.kegg.jp/>) (Kanehisa et al. 2021) and manually compared with the human (KEGG organism: hsa) metabolic pathways. Information of proteins involved in both the unique and common pathways was extracted from the UniProt (Proteome ID: UP000000793) (<https://www>

uniprot.org/) (Bateman 2019) database and NCBI database (RefSeq: NC_010079.1; <https://www.ncbi.nlm.nih.gov>) (O’Leary et al. 2016) for USA300_TCH1516.

Assessment of Essential Pathogenic Genes

Database of essential genes (DEG; <http://origin.tubic.org/deg/public/index.php/index>) contains genomic information from bacteria, archaea and eukaryotic organisms necessary for maintaining their lives (Luo et al. 2014). Currently, 30,878 essential bacterial genes are present in the database (Updated on 1st September 2020). To identify the essential proteins of the MRSA USA300_TCH1516 strain, the BLASTP analysis that is integrated with the DEG database, was performed. Proteins with e-value < 0.0001 and bit score > 100 were considered as essential proteins for bacteria (Jadhav et al. 2013).

Identification of Non-homologous Genes

Host proteins were avoided to circumvent side effects while searching for possible therapeutic targets. Initially, the metabolic pathway information of the host and pathogen were collected and compared manually. To determine the non-homologous genes, protein sequences were subjected to NCBI BLASTp server (<https://blast.ncbi.nlm.nih.gov/Blast.cgi>) (Boratyn et al. 2012). A similarity search of *S. aureus* essential genes was performed against the human proteome. Proteins with e-value < 0.005 and sequence similarity < 35% (Pearson 1995, 1996) were considered as non-homologous to the human host. This analysis is an essential determining step since it helps to avoid cross-reactivity with the host proteome for designing vaccines and drugs (Sarkar et al. 2012).

Identification of Subcellular Localization of Target Proteins

In general, extracellular, periplasmic and surface proteins are treated as potential vaccine targets. Additionally, the inner membrane and cytoplasmic proteins are considered as drug targets (Solanki et al. 2019). Therefore, subcellular localization screening was performed for all the resultant target proteins using PSORTb v3.0 server (<https://www.psорт.org/psортb/>) (Yu et al. 2010) and CELLO v2.5 server (<http://cello.life.nctu.edu.tw/>) (Yu et al. 2006). Predicted extracellular proteins were further cross-verified for their transmembrane domain using TMHMM v2.0 server (<http://www.cbs.dtu.dk/services/TMHMM/>) (Moller et al. 2001). The extracellular and surface-expressed proteins so obtained were further subjected to antigenicity checking.

Evaluation of Antigenicity of Extracellular and Surface-Expressed Proteins

Validating immunogenic protein targets is essential before vaccine designing. The VaxiJen v2.0 server (<http://www.ddg-pharmfac.net/vaxijen/VaxiJen/VaxiJen.html>) was used for computationally predicting the potential of a protein to induce antigenicity in the host where the threshold value was set to 0.4 (Doytchinova and Flower 2007). The target proteins with a higher value above the threshold limit were considered as immunogenic. The resultant antigenic proteins were then subjected to epitope mapping.

Prediction of Linear B-Cell Epitopes of Antigenic Vaccine Targets

Proteins obtained from VaxiJen v2.0 were analysed for linear B-cell epitope prediction. In general, peptide vaccines are better than whole organisms or large proteins because peptide fragments confer a highly targeted immune response and avoid unnecessary antigenic load. Peptide vaccine only includes antigenic epitope despite using the complete antigen protein (Li et al. 2014). Epitope identification is a costly and time-consuming process as it requires experimental screening of large datasets of potential epitope candidates. The B-cell epitope is a linear peptide fragment of the antigen that binds to the immunoglobulin or antibody (Sanchez-Trincado et al. 2017). B-cells recognize solvent-exposed antigens through the B-cell receptors (Jespersen et al. 2019). Protein sequences of vaccine targets were used to predict B-cell epitopes using, artificial neural network-based ABCpred server (<http://crdd.osdd.net/raghava/abcpred/>) (Saha and Raghava 2006), and three-dimensional structure-based BepiPred 2.0 server (<http://www.cbs.dtu.dk/services/BepiPred/>) (Jespersen et al. 2017) and IEDB antibody epitope prediction server (<http://tools.iedb.org/main/bcell/>) (Vita et al. 2019) with an epitope threshold setting of 0.51. The most common epitopes from the three servers were then selected as vaccine targets.

Druggability Analysis of Essential Non-homologous Proteins

The most reliable way to identify the druggability of proteins is to identify the similar proteins which can bind to the drug-like compound (Hajduk et al. 2005). Non-homologous essential proteins were searched against the DrugBank database to find out the FDA-approved drugs in the DrugBank database (<https://go.drugbank.com/>) (Wishart et al. 2018) using the inbuilt BLAST tool. Druggability analysis was performed for all the essential non-homologous protein targets with default search parameters (e-value < 0.00001). DrugBank

database contains a comprehensive molecular information about drugs, their mechanisms, their interactions and their targets. Based on this, hits found with DrugBank were considered as druggable targets with FDA-approved drugs, whereas others were considered as novel drug targets.

Protein–Protein Interactions (PPIs)

Peptidoglycan is the main component of *S. aureus* cell wall, a complex, three-dimensional mesh surrounding the entire cell (Vollmer et al. 2008). It maintains the cell shape, integrity and protects the bacteria; thereby, the biosynthetic machinery of peptidoglycan has been a preferred target for the discovery of antibacterials (Nikolaidis et al. 2014). To understand the involvement of proteins towards peptidoglycan biosynthesis, protein–protein interaction (PPI) studies were performed. Thus, the essential non-homologous proteins that were obtained from the previous analysis were accounted for PPI studies, and the peptidoglycan synthesis pathway was analysed further. This study provides information about their potential roles in metabolic, biological and functional aspects. Search Tool for the Retrieval of Interacting Genes/Proteins (STRING v11.0) (<https://string-db.org/>) (Szklarczyk et al. 2019) was used for mapping the interactions between non-homologous target proteins to create an intra-species protein–protein interaction network.

Selection of Crystal Structure and Fixing Missing Residues

Drug resistance is governed by genomic factors that are involved in cell wall metabolism (Berger-Bächli and Tschierske 1998); thereby, this study focused on targeting cell-wall biosynthesis proteins. Studies show that Staphylococcal FemXAB family proteins play a vital role in the later stages of peptidoglycan biosynthesis and may serve as suitable targets for therapeutic agents (Monteiro et al. 2019). Structure-based virtual screening requires the crystal structure of the target protein. The crystal structure of the staphylococcal FemA protein was retrieved from the Protein Data Bank (<https://www.rcsb.org/>) (Goodsell et al. 2020) under code 1LRZ (Benson et al. 2002). The missing residues 209–220 and 413–420 of FemA were fixed by Robetta (Kim et al. 2004), phyre2 (Kelley et al. 2015) and SWISS-MODEL (Waterhouse et al. 2018). The quality of the model structures was validated using QMEAN (Qualitative Model Energy Analysis) (<https://swissmodel.expasy.org/qmean/>) (Benkert et al. 2011), prosa (<https://prosa.services.came.sbg.ac.at/>)

(Wiederstein and Sippl 2007) and PROCHECK (Laskowski et al. 1993). The best model was optimized by 200 steps steepest descent energy minimization using the Swiss-PdbViewer (Guex et al. 2009).

Structure-Based Virtual Screening

The active site of FemA was analysed and screened for drug identification (Benson et al. 2002). The receptor structure was prepared for virtual screening by adding the polar hydrogen atoms and Kollman charges. One thousand nine hundred and eighteen FDA-approved drugs were downloaded in SDF file format from DrugBank Database for screening. No ligand–bound FemA crystal structure is available in Protein Data Bank (PDB). So, it was necessary to proceed with the active site pocket for virtual screening. During ligand preparation, the prepareligand4.py python script supplied by the AutoDock developers (Morris et al. 2009), was used. Open Babel was used to convert all drug compound files into PDBQT format (O’Boyle et al. 2011). A receptor grid-box was generated with grid box dimensions of 90 Å × 90 Å × 90 Å with centre at x = 42.075, y = 62.493, z = 90.597. AutoDock Vina (Trott and Olson 2009) was used for virtual screening of processed drugs against *S. aureus* FemA. Further, the top ten drugs obtained from the virtual screening were accounted for docking analysis using AutoDock 4.2 (Morris et al. 2009).

Molecular Docking

The receptor was subjected to pre-processing to be used in AutoDock 4.2 (Morris et al. 2009) for docking. Polar hydrogens followed by Kollman charges were added to FemA. Non-polar hydrogens were merged, and Gasteiger charges were added to the selected ligands using AutoDock 4.2. The same gridbox with a centre at x = 42.075, y = 62.493, z = 90.597 and dimensions of 90 Å × 90 Å × 90 Å with a grid space of 0.375 was used for molecular docking using the AutoDock 4.2 tool, which was earlier used in virtual-screening. Lamarckian Genetic Algorithm (GA) was used to perform a total of 10 runs. Autodock estimates free energy of binding (ΔG), which is the sum of the intermolecular energy (vdW + H-bond + desolv Energy + Electrostatic Energy), the internal energy, and the torsional energy minus the unbound system’s internal energy (Morris et al. 2008). AutoDock calculates the inhibition constant (K_i) value using the equation [$K_i = \exp(\Delta G/(R \cdot T))$]. The final result of docking was visualized by UCSF Chimera v1.15 (Pettersen et al. 2004), and the structures were analyzed manually by LigPlot⁺ (Laskowski and Swindells 2011) to decrypt the receptor–ligand interactions.

Results

Genomic Features of Pathogenic Strains

S. aureus USA300_TCH1516 strain (NC_010079) had a circular genome of ~2.87 Mbp (Supplementary Fig. 1) with ~32.7% GC content also contained 2,763 coding genes (Supplementary Table 1). The genome size of 14 strains ranged between 2.7 and 2.9 Mbp, and their GC content varied between 32.7 and 32.9% (Supplementary Table 1). IslandViewer4 presented the respective positions of curated virulence factors, homologs of virulence factors, curated resistance genes, homologs of resistance genes in *S. aureus* USA300_TCH1516 based on codon usage, dinucleotide bias and phylogenetically related genome information. Genome island visualization of all fourteen strains was in the supplementary document (Supplementary Fig. 1).

Pathogenic USA300 Strain has 29 Unique Pathogenic Pathways

The KEGG database contained 337 metabolic pathways from human and 105 metabolic pathways from *S. aureus* USA300_TCH1516. Out of the 105 metabolic pathways, 29 pathways were found to be unique to *S. aureus* USA300_TCH1516 (Supplementary Table 2), and the remaining 76 pathways were shared by both pathogen and host (Supplementary Table 3).

Identification of 198 Essential Non-homologous Pathogenic Proteins

Out of the 295 essential proteins present in the DEG database, 198 essential proteins were identified as non-homologous to the host, thereby defined as “NON-HOST” (Supplementary Table 4). Essential proteins possess a significant role in the pathogenicity and survival of the organism (Lewin et al. 2019). So, these 198 essential non-homologous proteins are very crucial for *S. aureus*-mediated pathogenesis. These proteins can be exploited as potential therapeutic candidates.

Identification of Eight Extracellular Proteins as Potential Vaccine Targets

Sub-cellular localization of protein plays a vital role in understanding the protein function, providing breakthrough information for drug designing and discovery. A total of 190 cytoplasmic and inner membrane proteins were identified as drug targets, and eight extracellular proteins were identified as potential vaccine targets (Supplementary Table 4).

Identification of Seven Antigenic Extracellular Proteins

Antigenicity is the ability to be recognized explicitly by the antibodies generated due to the immune response to the given substance (Ilinskaya and Dobrovol'skaia 2016). VaxiJen v2.0 provided the antigenicity information of the epitopes to understand the immunomodulatory effect of epitopes that were identified from immunogenic regions. Epitopes with a higher than VaxiJen cut-off value (0.4) were selected as potential epitopes, and their antigenicity values range from 0.5 to 0.8 (Supplementary Table 5). Out of 8 extracellular proteins, seven proteins except Diadenylate cyclase (Q2FW92) meet the threshold value (>0.4), and possess antigenicity (Table 2).

Prediction of Linear B-Cell Epitopes in Extracellular Proteins

A total of seven antigenic extracellular proteins were identified from the bacterial membrane of *S. aureus* USA300_TCH1516. Two cell division proteins (Q2FZ91, Q2FZ95), two penicillin-binding proteins (Q2FZ94, Q2FYI0) of bacterial cell wall, pentose phosphate pathway component phosphoglucomutase (Q2FE11), glycerolipid metabolism pathway component lipoteichoic acid synthase (Q2FIS2) and an uncharacterized protein; are the vaccine targets onto which B-cell epitopes were mapped (Table 1). Predicted epitopes fall into the solvent-accessible part of the proteins recognized by respective antibodies (Jespersen et al. 2019). Here, five anticipated epitopes are the mixtures of secondary structures such as helix and coil (cell division protein DivIB, penicillin-binding protein-1 and phosphoglucomutase), β -sheet and coil (penicillin-binding protein-2). However, lipoteichoic acid synthase epitope lies only in coil structure, and cell division protein ftsL lies only in a helical structure. At most penicillin-binding protein-2 and lipoteichoic acid synthase crystal structures are available in Protein DataBank with PDB ID: 3DWK and 2W5Q, respectively.

Identification of 53 Bacterial Essential Non-homologous Proteins as Targets for Drug Repurposing

This study considered the importance of essential non-homologous characteristics of proteins, thereby reduced the number of prioritized sequences as therapeutic targets. Therefore, the comparative computational genomics approach was implemented here to shortlist potential drug targets stepwise. Sequence similarity search with all

Table 1 Vaccine targets with mapped epitopes against *S. aureus* USA300_TCH1516 strain

Sl.	Protein Name	Gene	UniProt	Pathway	VaxiJen value	Epitope	Structure
1	Cell division protein DivIB	divIB	Q2FZ91	Sax04112 Sulfur relay system	0.70	NNHVSTSKI	No
2	Hypothetical protein	–	Q2G0R4	Unknown	0.68	RDDYYLSNKGE	No
3	Penicillin-binding protein 1	pbpA	Q2FZ94	Sax00550 Peptidoglycan biosynthesis Sax01100 Metabolic pathways Sax01501 β -Lactam resistance	0.63	KMKSWYERFGFGKS	No
4	Penicillin-binding protein 2	pbp2	Q2FYI0	Sax00550 Peptidoglycan biosynthesis Sax01100 Metabolic pathways Sax01501 β -Lactam resistance	0.58	SSYQVDGSTFRNYDTK	3DWK
5	Lipoteichoic acid synthase	ltaS	Q2FIS2	Sax00561 Glycerolipid metabolism Sax01100 Metabolic pathways	0.50	KTFWNRDQVYKHFG	2W5Q
6	Phosphoglucomutase	pgcA	Q2FE11	Sax00010 Glycolysis/Gluconeogenesis Sax00030 Pentose phosphate pathway Sax00230 Purine metabolism Sax00500 Starch and sucrose metabolism Sax01100 Metabolic pathways Sax01110 Biosynthesis of secondary metabolites	0.47	FSSVQSANPEDHRAFD	No
7	Cell division protein FtsL	ftsL	Q2FZ95	Unknown	0.75	IDKQSSENSA	No

Seven extracellular proteins are selected for epitope prediction after checking their antigenicity

available drug targets in the DrugBank database provided 53 prioritized drug targets within the USA300_TCH1516 proteome (Table 2). FDA-approved drugs for which the experimental evidence of binding with proteins similar to *S. aureus* was available in the DrugBank database. All these prioritized targets belonged to the common metabolic pathways of MRSA, such as fatty acid biosynthesis (Q93QD4, A8Z088, Q6GI75), folate biosynthesis (Q2FY51, Q2G0Q7, Q2FXR9), peptidoglycan biosynthesis (Q2FZ94, Q2FYI0, A8Z4Y6, A8Z012), and ribosome (Q2FEP5, A8YZP4, A8Z2N6, A8YZN7), etc.

Peptidoglycan Biosynthesis Proteins as Drug Targets

Cellular and molecular life depends on a complex network of interactions between the biomolecules. Among these interactions, protein–protein associations are fundamental due to their versatility, specificity and adaptability. Resultant 198 essential non-homologous proteins generated a complex interaction network for *S. aureus* USA300_TCH1516 proteins (Supplementary Fig. 2). This study was emphasized on proteins involved with antibiotic resistance, thereby the peptidoglycan biosynthesis protein cluster was exclusively analysed (Fig. 2). In this network, it was found that penicillin-binding protein 2 (pbp2) was interacting with the staphylococcal FemA (P0A0A5), FemB (P0A0A8) and the FemX (Q2FEM9). Pbp2 (Q2FYI0) was also found to be

interacting with murB to murG, mraY and ddl proteins in the multi-node network. Ddl and Mur family proteins are crucial for peptidoglycan synthesis, thereby found interacting with pbpA (Q2FZ94), another penicillin-binding protein encoded by the *pbpA* gene. Protein pbp2 was indirectly involved in Biological processes (GO) cell division (GO: 0051301) and cell cycle mechanisms (GO: 0007049). Mur family proteins participated in the peptidoglycan biosynthesis process (GO: 0009252), regulation of cell shape (GO: 0008360), and cell wall organization (GO: 0071555). The mraY (A8Z3M3) and ddl (A8Z4Y6) proteins were crucial players of the peptidoglycan biosynthesis pathway (00550) and the vancomycin resistance pathway (01502). Both pbp2 and pbpA proteins manifested a combined role in peptidoglycan biosynthesis (00550) and β -lactam resistance (01501).

Homology Model of Staphylococcal FemA

Phyre2 used a one-to-one threading approach, whereas Robetta utilized comparative modelling using the crystal structure of FemA (PDB: 1LRZ). The best structure was provided from each server based on their scoring function. Each structure was checked for its reliability based on QMEAN score, Prosa Z-score and Ramachandran plot analysis. A more positive QMEAN score indicated a better model after evaluating the quality of a protein model. Prosa evaluated the model structure quality by scanning and comparing them

Table 2 Predicted drug targets against *S. aureus* USA300_TCH1516 strain

Sl No.	UniProt	Protein name	Sl No.	UniProt	Protein name
1	A8Z2L6	Acetyl-coenzyme A carboxylase carboxyl transferase subunit β (accD)	28	Q2FYI0	Penicillin-binding protein 2 (pbp2)
2	Q2G268	Coenzyme A biosynthesis bifunctional protein (coaBC)	29	Q2G2Q2	Riboflavin biosynthesis protein
3	Q2FZY5	Cysteine desulfurase	30	A8YZN7	50S ribosomal protein L10 (rplJ)
4	A8Z4Y6	D-alanine–D-alanine ligase (ddl)	31	Q2FEP6	50S ribosomal protein L16 (rplP)
5	Q93QD4	Malonyl CoA-acyl carrier protein transacylase FabD (fabD)	32	Q2FEP4	50S ribosomal protein L22 (rplV)
6	A8Z088	3-oxoacyl-[acyl-carrier-protein] synthase 3 FabH (fabH)	33	Q2FER5	DNA-directed RNA polymerase subunit alpha (rpoA)
7	Q6GI75	Enoyl-[acyl-carrier-protein] reductase [NADPH] FabI (fabI)	34	A8YZP0	DNA-directed RNA polymerase subunit β (rpoB)
8	A8Z536	Isopentenyl-diphosphate delta-isomerase Fni (fni)	35	Q2FEP5	30S ribosomal protein S3 (rpsC)
9	Q2G0Q5	2-amino-4-hydroxy-6-hydroxymethyl-dihydropteridine pyrophosphokinase	36	Q2FEN8	30S ribosomal protein S10 (rpsJ)
10	Q2G0Q7	Dihydropteroate synthase	37	A8Z333	30S ribosomal protein S13 (rpsM)
11	Q2FXR9	Dihydrofolate synthase (folC)	38	P0A0J0	RNA polymerase sigma factor SigA (sigA)
12	P0A040	Glutamine synthetase (glnA)	39	Q2FZY7	Fe-S cluster assembly ATPase SufC (sufC)
13	A8Z4T2	60 kDa chaperonin GroEL (groL)	40	Q2FJ01	Teichoic acids export ATP-binding protein TagH (tagH)
14	Q5HJZ0	DNA gyrase subunit A (gyrA)	41	Q2G041	Thioredoxin-disulfide reductase
15	Q2FYG6	Heptaprenyl diphosphate syntase component II	42	P0A017	Dihydrofolate reductase (folA)
16	A8Z012	UDP-N-acetylenolpyruvoylglucosamine reductase (murB)	43	Q2FIB3	Glucose-6-phosphate isomerase (pgi)
17	A8Z4D3	Nicotinate-nucleotide adenyltransferase (nadD)	44	A8YZP4	30S ribosomal protein S7 (rpsG)
18	A8Z2S7	Ammonia-dependent NAD (+) synthetase (nadE)	45	A8Z1J1	D-alanine–D-alanyl carrier protein ligase (dltA)
19	Q2G078	Ribonucleoside-diphosphate reductase subunit alpha (nrdA)	46	Q2FY51	Dihydrolipoyl dehydrogenase
20	Q2G077	Ribonucleoside-diphosphate reductase subunit β (nrdF)	47	Q2FXN4	NADP-dependent isocitrate dehydrogenase
21	A8Z002	Ribonucleotide-diphosphate reductase subunit gamma (nrdI)	48	Q2FE05	UTP–glucose-1-phosphate uridylyltransferase (gtaB)
22	Q2G0W2	NADH dehydrogenase subunit 5	49	P64126	Ferrochelatase (cpfC)
23	Q2FYS4	DNA topoisomerase IV subunit A (parC)	50	Q2FE11	Phosphoglucosyl mutase (pgcA)
24	P0C1S7	DNA topoisomerase IV subunit B (parE)	51	A8Z2N6	30S ribosomal protein S4 (rpsD)
25	Q2FZ94	Penicillin-binding protein 1 (pbpA)	52	A8Z343	30S ribosomal protein S8 (rpsH)
26	A8Z1R9	Phenylalanine–tRNA ligase subunit alpha (pheS)	53	A8Z344	30S ribosomal protein S14 type Z (rpsZ)
27	Q2FHU2	Phenylalanine–tRNA ligase subunit β (pheT)			

Essential non-homologous proteins are introduced to the DrugBank database search whether FDA-approved drugs are available for which the experimental evidence of binding with proteins similar to the target proteins

with the crystal structures available in PDB. Based on the QMEAN and Prosa Z-score, the best model was predicted by Robetta (Supplementary Table 6).

Drug Binding with Staphylococcal FemA

Top ten hits were obtained from virtual screening based on their binding energies to the receptor (Fig. 3). All drugs had binding energy of more than -11.0 kcal/mol

(Table 3). These repurposing drugs are used to treat a wide range of diseases such as hyponatremia, migraine headaches and many types of cancers; Irinotecan in colorectal cancer (Fujita et al. 2015), Conivaptan in hyponatremia (Ghali 2009), Dutasteride in benign prostatic hyperplasia (Wu and Kapoor 2013), Midostaurin in acute myeloid leukaemia (Fischer et al. 2010), Rupatadine in symptomatic relief (Keam and Plosker 2007), Ergotamine, Rimegepant and Dihydroergotamine in migraine (Tfelt-Hansen 2000;

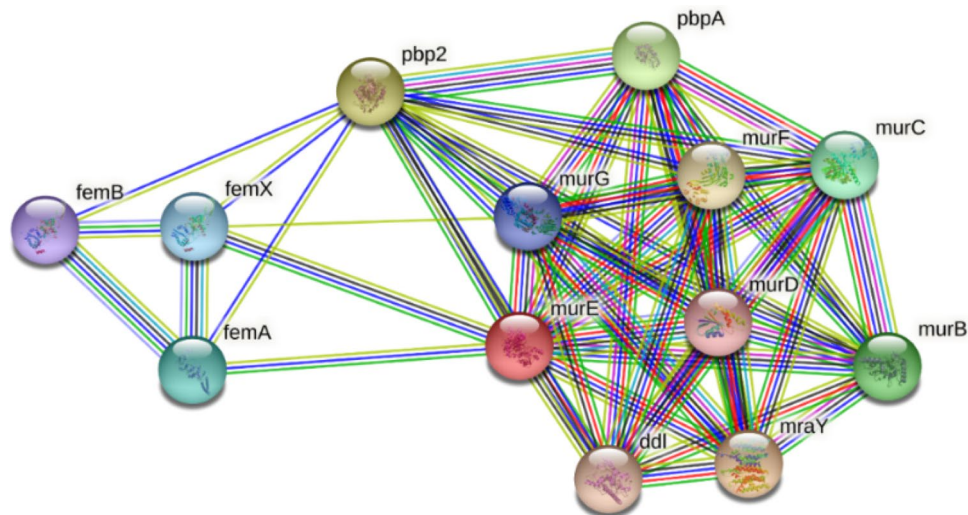


Fig. 2 The protein–protein interaction (PPI) network of essential bacterial non-homologous proteins involved with peptidoglycan biosynthesis. Penicillin-binding proteins (pbp2, pbpA) are found interacting directly or indirectly with Ddl, FemXAB and Mur-family proteins to maintain the cell-wall integrity and render antibiotic resistance. The FemA protein contributes a high-level of methicillin resistance in *S.*

aureus, thereby could be a potential therapeutic target to combat the MRSA USA300. Black lines indicate the co-expression, the blue line indicates the gene co-occurrence, the green line indicates gene neighbourhood, the red line indicates gene fusions. Figure is generated using STRING (Color figure online)

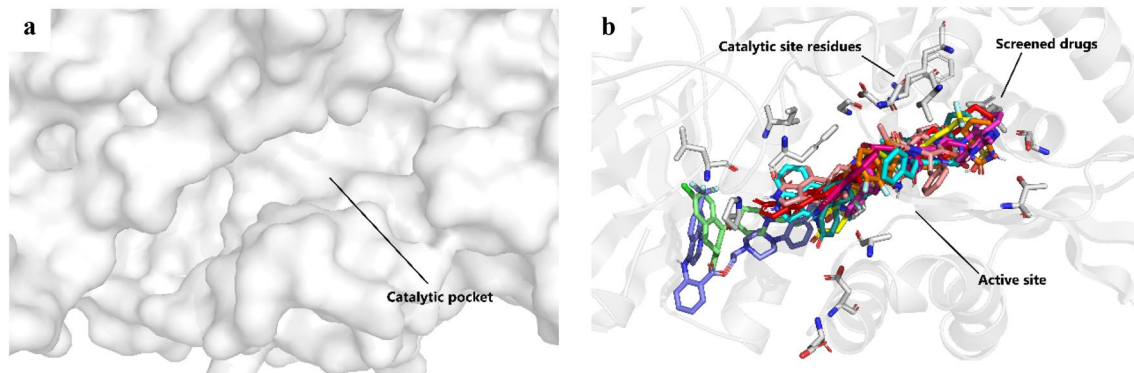


Fig. 3 The crystal structure of staphylococcal FemA curated from Protein Data Bank (PDB ID: 1LRZ). **a** Surface model of the catalytic pocket. **b** Distribution of screened FDA-approved drugs in the catalytic pocket after the virtual screening. Grey ribbon represents the

active site region of the protein, and grey sticks correspond to the catalytic pocket residues. Ten screened drugs are represented using the coloured sticks of red, lime green, forest green, salmon, magenta, hot pink, yellow, blue, marine and cyan (Color figure online)

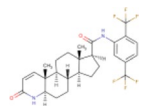
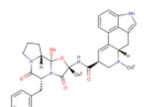
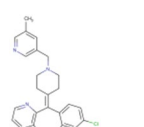
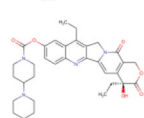
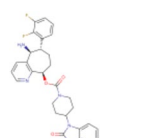
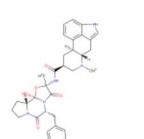
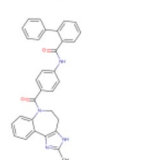
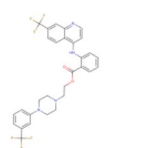
Lipton et al. 2019; Schürks 2009) and Antrafenine as an anti-inflammatory (Berry et al. 1983).

Analysis of Molecular Interactions Between FemA and Drugs

AutoDock 4.2 generates a bunch of energy values (binding energy, ligand efficiency; inhibition constant; intermolecular energy; Van der Waals, electrostatic and total internal energy) using a Lamarckian program. The binding energy and inhibition constant (Ki) indicate the overall strength of a given

predicted interaction calculated by AutoDock 4.2 (Matossian et al. 2014). Molecular docking furnished further insights into the ligand–receptor interactions by providing information about the binding affinity as well as inhibition constant (Ki) for all 10 FDA-approved drugs. Docking results were analyzed to comprehend their interaction with amino acids using LigPlot⁺ (Table 4). Structure-based virtual screening and docking were attempted focusing on the pocket of 1B domain of staphylococcal FemA that is the only active site according to the literature (Benson et al. 2002). While analyzing the affinity of drugs for the receptor, it was found that Irinotecan possesses binding

Table 3 List of repurposing drugs targeting *S. aureus* femA protein

DrugBank code	Drug name	AutoDock Vina ΔG (kcal/mol)	AutoDock 4.2 ΔG (kcal/mol)	AutoDock 4.2 Inhibition constant (Ki) (nM)	Chemical structure
DB01126	Dutasteride	– 11.70	– 9.88	57.58	
DB06595	Midostaurin	– 11.50	– 10.62	16.51	
DB14703	Dexamethasone metasul- fobenzoate	– 11.50	– 10.75	13.15	
DB00696	Ergotamine	– 11.30	– 10.54	18.88	
DB11614	Rupatadine	– 11.30	– 10.21	32.78	
DB00762	Irinotecan	– 11.20	– 11.58	3.23	
DB12457	Rimegepant	– 11.20	– 9.97	49.25	
DB00320	Dihydroergotamine	– 11.10	– 10.10	39.67	
DB00872	Conivaptan	– 11.10	– 10.34	26.25	
DB01419	Antrafenine	– 11.10	– 7.36	4050	

These FDA-approved drugs are already clinically proven to treat various cancers, migraine and leukaemia, etc. Docking with AutoDock 4.2 renders the information about affinity as well as inhibition constant (Ki) for all 10 FDA-approved drugs towards the FemA protein.. Out of 10 drugs, 7 drug molecules show binding energy of more than -10.0 kcal/mol

energy (B.E.) of – 11.58 kcal/mol with the FemA, the highest binding energy among all selected drugs (Table 3). Usually, the smaller the inhibition constant (Ki) value corresponds to a

more significant binding affinity, and interestingly Irinotecan also manifests the lowest inhibition constant (Ki). Besides, the highest number of hydrophobic interactions and the formation

Table 4 Interactions between amino acids and identified drugs predicted through the analysis of AutoDock 4.2 docking results using LigPlot⁺

Amino acids	Dutasteride	Midostaurin	Dexamethasone metasulfobenzoate	Ergotamine	Rupatadine	Irinotecan	Rimegepant	Dihydroergotamine	Conivaptan	Antrafenine
Phe149	✓	✓	✓	✓	✓	✓	✓	✓	✓	✓
Asp150				✓	✓	✓		✓	✓	
Pro151				✓		✓		✓	✓	
Leu153			✓	✓				✓	✓	
Gln154			✓		✓					
Ile155			✓	✓	✓			✓		
Lys215		✓				✓		✓		
Ala216		✓				✓	✓	✓		✓
Phe217	✓	✓		✓		✓		✓		✓
Ala218		✓						✓		
Asp221		✓			✓					
Ser314					✓					
Ala315					✓					
Tyr327	✓	✓	✓	✓	✓	✓	✓	✓	✓	✓
Tyr328	✓	✓	✓	✓	✓	✓	✓	✓	✓	✓
Ala329	✓	✓		✓	✓	✓	✓	✓		✓
Gly330	✓	✓		✓	✓	✓	✓	✓		✓
Gly331	✓					✓	✓	✓		
Thr332	✓					✓	✓	✓		
Ser342	✓					✓	✓			
Gln346	✓	✓	✓			✓				
Phe363	✓	✓	✓	✓	✓	✓	✓	✓	✓	
Tyr364	✓	✓	✓	✓	✓	✓	✓	✓	✓	✓
Gly365	✓		✓		✓	✓	✓	✓	✓	
Asp376		✓		✓				✓	✓	
Val379		✓	✓	✓				✓	✓	✓
Phe382			✓							
Lys383	✓	✓	✓		✓	✓	✓	✓	✓	✓

Phe149, Tyr327, Tyr328, Phe363, Tyr364 and Lys383 are the most common amino acids that show interactions with the highest number of the drugs. Along with, Tyr328 and Lys383 showed the highest hydrogen bond interactions. All interacting amino acids that bind to the drugs are part of the active site cavity

of four hydrogen bonds (H-bond), implying Gly330, Thr332, Ser342 and Gln346 between drug-receptor, probably justified the higher binding energy among all the predicted drugs (Figs. 4a and 5a). Dexamethasone metasulfobenzoate showed the second-highest binding energy, i.e., -10.75 kcal/mol, with a lower inhibition constant value (Table 3). Other than Irinotecan, Dexamethasone metasulfobenzoate also possessed four H-bonds engaging Leu153, Tyr327, Gly365 and Lys383, indicating higher binding energy (Figs. 4b and 5b). Midostaurin exhibited the binding energy of -10.62 kcal/mol though a single H-bond formed with the receptor implying Lys383, but the higher number of hydrophobic interactions explained the higher binding energy in drug–protein interaction (Figs. 4c and 5c). Molecular interaction analysis showed that Ergotamine possessed three H-bonds involving Asp150, Tyr328 and Lys383, and several hydrophobic interactions (Figs. 4d and 5d) leading to the binding energy of -10.54 kcal/mol. Convivaptan possessed four H-bonds involving the residues Ala216, Tyr364, Gly365 and Lys383 with a binding energy of -10.34 kcal/mol (Supplementary Figs. 6a and 7a). Rupatadine showed the binding energy of -10.21 kcal/mol, engaging

Tyr328, Phe363 and Lys383 for H-bonding and several other residues in hydrophobic interactions (Supplementary Figs. 6b and 7b). In the case of Dihydroergotamine, three hydrogen bonds with the residues Asp150, Tyr328 and Gly330 and several hydrophobic interactions togetherly helped to achieve the binding energy of -10.10 kcal/mol (Supplementary Figs. 6c and 7c). Rimegepant possessed two H-bonds involving the residues Tyr328 and Lys383 and several hydrophobic interactions that combinedly showed the binding energy of -9.97 kcal/mol (Supplementary Figs. 6d and 7d). Dutasteride manifested two hydrogen bonds implying the residues Tyr328 and Ser342 of FemA, and possessed the binding energy of -9.88 kcal/mol (Supplementary Figs. 6e and 7e). Antrafenine exhibited two H-bonds engaging Tyr328 and Lys383 and less hydrophobic interactions, thereby showing the binding energy of -7.36 kcal/mol (Supplementary Figs. 6f and 7f), which is the lowest among all. Visual analysis of docked complexes displayed that Phe149, Tyr327, Tyr328, Phe363, Tyr364 and Lys383 are the most common amino acids that show interactions with most of the drugs (10, 10, 10, 9, 10 and 9 drugs respectively) and followed by Ala329, Gly330

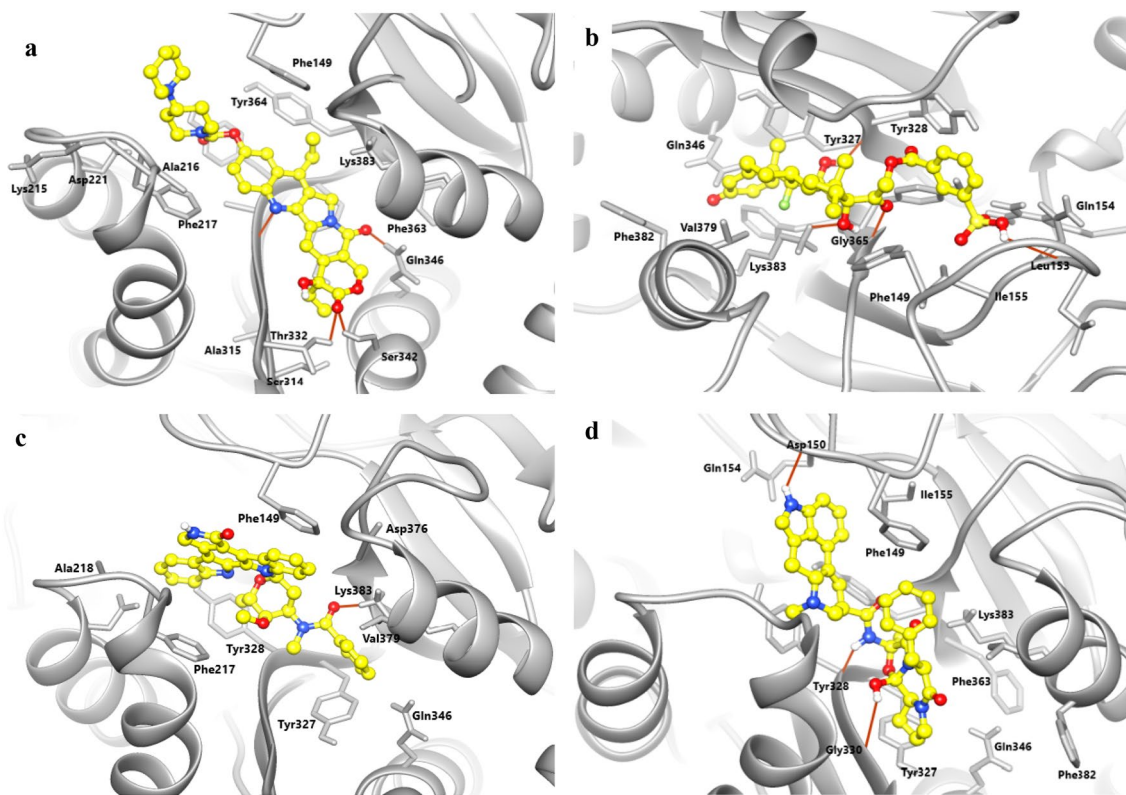
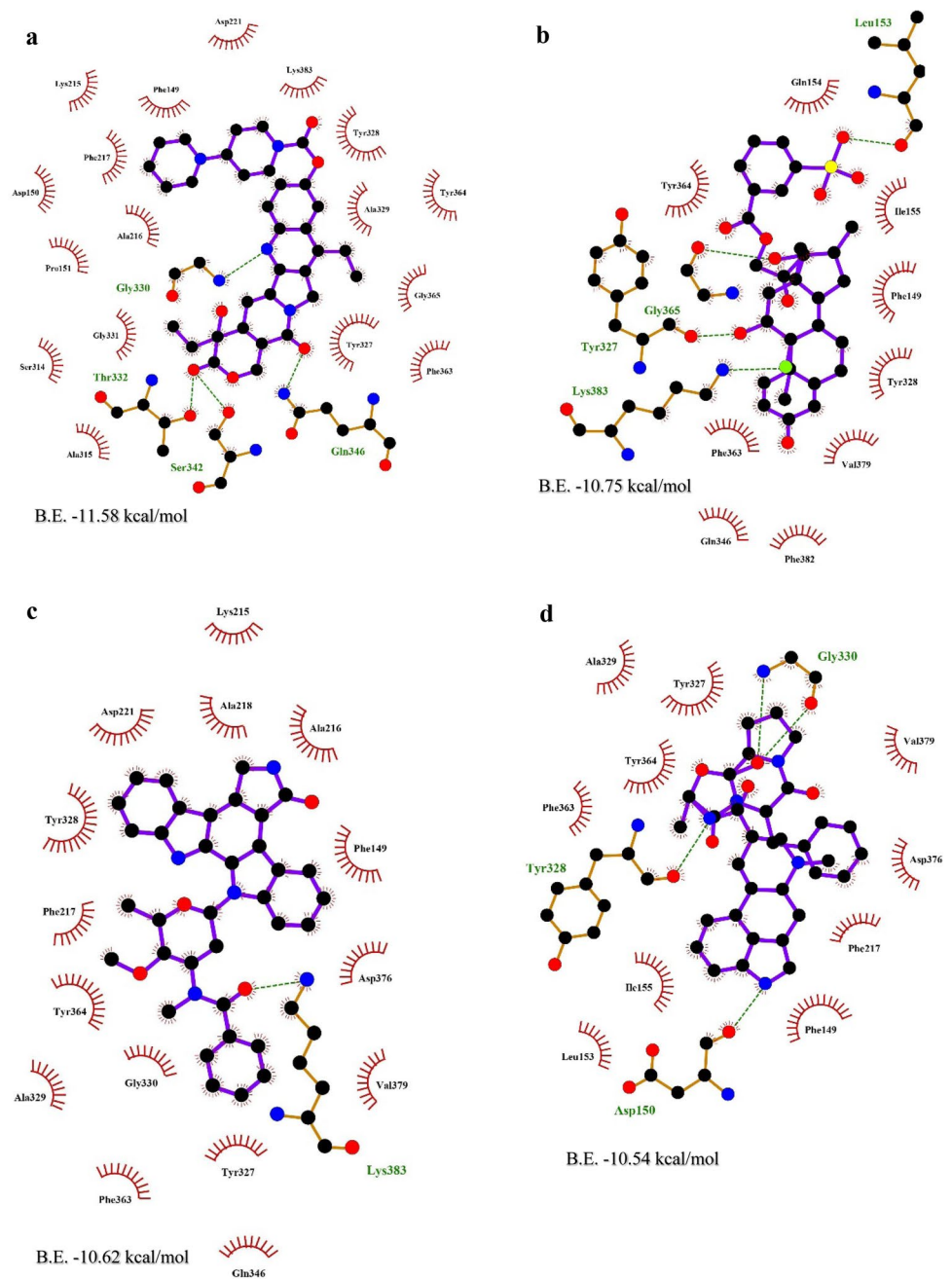


Fig. 4 Docking of *S. aureus* FemA protein with ten FDA-approved drugs that are selected from the structure-based virtual screening. **a** Molecular interactions of Irinotecan with FemA protein. **b** Molecular interactions of Dexamethasone metasulfobenzoate with FemA protein. **c** Molecular interactions of Midostaurin with FemA protein. **d** Molecular interactions of Ergotamine with FemA protein. Grey rib-

bons represent the FemA protein, whereas yellow ball and stick models correspond to the drug molecules binding to the only active site. Hydrogen bonds between receptor and protein are represented using orange lines, and amino acids involved in the interaction are labelled. Figures are generated using UCSF Chimera v1.15 (Color figure online)

Fig. 5 Visual representation of hydrogen bonds and hydrophobic interactions of selected drug compounds with FemA protein using LigPlot⁺. **a** Irinotecan. **b** Dexamethasone metasulfobenzozate. **c** Midostaurin. **d** Ergotamine. The olive green dotted lines represent the hydrogen bond, whereas brick red stellations correspond to the hydrophobic interactions. Olive green labelled amino acids involve hydrogen bonding and amino acids with brick red stellations representing the hydrophobic interacting residues in respective ligand–receptor connection surfaces (Color figure online)



and Gly365 (8, 7 and 7 drugs respectively). Besides, Tyr328 and Lys383 showed the highest hydrogen bond interactions. Out of 10 drugs, 7 drug molecules possessed binding energy of more than -10.0 kcal/mol (Table 3). All interacting amino acids binding to the drugs were found to be accumulated in the active site cavity. It was observed that the lower the K_i concentration, the higher the binding energy towards the receptor. And low-affinity binding (high K_i level) implied that a relatively high ligand concentration was required for interaction. Besides, hydrophobic interactions were abundant in the ligand–receptor binding, and all hydrophobic residues were part of domain 1B, the only active site of FemA.

Discussion

Several significant variants of CA-MRSA in the spatial and temporal population structures distributed globally with different clones dominate different regions globally. But USA300, a multi-locus sequencing (MLST) sequence type (ST) 8-MRSA-IV strain, is relentlessly found worldwide. The CA-MRSA clone ST8 increases virulence in the animal model and clinical incidents of several diseases (Chua et al. 2014). Even in vitro studies showed increased cytotoxicity of these clones against human macrophages (Laabei et al. 2015). *Staphylococcus aureus* is very notorious for its ability

to become resistant to antibiotics. Unfortunately, very few antibiotics have been introduced in the past 30 years representing novel chemical classes (Silver 2011). The resistance rates of *S. aureus* and multidrug-resistant strains are increasing gradually, making the clinical anti-infective treatment more difficult. The prospects for badly-needed new drugs to combat against staphylococcal bacteremia with novel mechanisms of action need to be assessed. For broader success, vaccine coverage is crucial to interrupt disease transmission.

Virulent factors and essential proteins of *S. aureus* USA300_TCH1516 and USA300_FPR3757 of USA300 lineage are reported to date. USA300_TCH1516 isotype represents the hypervirulent strain of MRSA USA300 lineage (Coe et al. 2019). Understanding the evolutionary relationships among pathogenic genomes is vital to target the virulent factors of the methicillin-resistant *S. aureus*. BLASTn analysis shows that the genomic similarity among all these strains ranges between 98 and 100% (Table 1). USA300_TCH1516 possesses 2920 genes and 2763 proteins though *S. aureus* JH1 hosts the highest number of genes and proteins (2957 genes, 2808 proteins) among all pathogenic *S. aureus* strains. Besides, the RF122 strain possesses the smallest gene size, genes and proteins during comparison, but interestingly RF122 contains the highest number of pseudogenes (Supplementary Table 1). This study identifies 29 unique pathways such as streptomycin biosynthesis, peptidoglycan biosynthesis, β -lactam resistance, vancomycin resistance, two-component system and quorum sensing etc. Other than that, 76 common pathways are also identified, which are shared by USA300_TCH1516 strain and human. It is well known that essential proteins possess a significant role in the pathogenicity and survival of the organism (Lewin et al. 2019). Hence, the objective of this study lies in finding out the essential genes of pathogenic *S. aureus* that have significant dissimilarity with the human genome. The DEG database contains information about 295 essential pathogenic genes for the *S. aureus* USA300_TCH1516 strain. Avoiding the cross-reactivity of potential therapeutics against human proteins is highly preferred. Upon sequence alignment of 295 essential proteins with the human proteome, 198 pathogenic proteins have been identified that are non-homologous to the host (Supplementary Table 2). Several cell division proteins, ribosomal proteins, uncharacterized proteins, cell-wall biosynthesis proteins and proteins associated with DNA replication are recognized by this study. Among these, only WalR (A8YYU1), a transcriptional regulatory protein, belongs to the unique metabolic pathway (Two-component system; sax02020), thereby all other essential non-homologous proteins share common metabolic pathways with the human. All these essential non-host proteins are appraised as potential therapeutic targets towards an antibiotic approach.

This work focuses on identifying potential drug targets along with immunogenic vaccine targets. Sub-cellular

localization of protein plays a significant role in understanding the protein functions essential for therapeutics discovery and development (Caragea et al. 2010). Extracellular, periplasmic and surface proteins are considered potential vaccine targets, whereas inner membrane and cytoplasmic proteins are considered drug targets (Solanki et al. 2019). Several bacterial systems are recently targeted for epitope mapping with this approach (Ain et al. 2018; Hizbullah et al. 2018; Ehsan et al. 2018). In this context, the sub-cellular localization study defines 175 cytoplasmic proteins, 15 inner membrane proteins and 8 extracellular proteins (Supplementary Table 2). Vaccine development requires the prediction of the B-cell epitope, the antigen portion that binds to the antibody. With that purpose, immunogenicity verification of B-cell epitopes is the first stage in vaccine design and development (Zaharieva et al. 2019). Out of 8 extracellular proteins, 7 proteins except for Diadenylate cyclase (Q2FW92) meet the threshold value (> 0.4), and hence they possess antigenicity (Supplementary Table 5). Usually, B-cell epitope length varies from 5 to 20 amino acids. Predicted epitopes have the length ranging from 9 to 16 residues, and fall in the exposed region of extracellular proteins, which are the main criteria for being considered as epitopes. The cell division proteins (Q2FZ91, Q2FZ95), penicillin-binding proteins (Q2FZ94, Q2FY10) of bacterial cell wall, pentose phosphate pathway component phosphoglucomutase (Q2FE11), and glycerolipid metabolism pathway component lipoteichoic acid synthase (Q2FIS2) are essential for the survival of the pathogen and thereby predicted to have B-cell epitopes in this study. Penicillin-binding proteins (Q2FZ94, Q2FY10) are involved in the peptidoglycan biosynthesis and β -Lactam resistance and metabolic pathways. Phosphoglucomutase (Q2FE11) is found present in glycolysis, purine metabolism, pentose phosphate pathway and metabolic pathways etc. It is observed that the majority of these proteins (Penicillin-binding proteins, phosphoglucomutase and lipoteichoic acid synthase) are important players of metabolic pathways. However, pathway information is not available for cell division protein FtsL (Q2FZ95) and an uncharacterized protein (Q2G0R4). Phosphoglucomutase and penicillin-binding proteins have been considered as potential vaccine targets in other bacterial systems (Buchanan et al. 2005; Rashid et al. 2017; Shah et al. 2021). Although immunoinformatics approaches were established to identify potential epitopes from the pathogens, some computationally predicted epitopes may not be optimally immunogenic in vivo. Therefore, the requisition is to test the predicted epitopes to ensure that they can generate B-cell responses.

The druggability of each non-host essential protein of *S. aureus* USA300_TCH1516 is identified by sequence similarity to the targets of FDA-approved drugs using the DrugBank database. This approach reduces the testable proteins

to 53 and delivers a list of FDA-approved drugs from the DrugBank that can bind to the target proteins of the pathogen. However, the protein sequence similarity search has limitations in such a way that it does not assure the binding regions identicalness of the identified similar proteins. Thereby, predicted targets are further needed to be validated through clinical experiments. Many specific drug targets that are identified from the common metabolic pathways like cysteine desulfurase (Q2FZY5), D-alanine-D-alanine ligase (A8Z4Y6), Malonyl CoA-acyl carrier protein transacylase (Q93QD4), Dihydropteroate synthase, Dihydrofolate reductase (Q2G0Q7), Glutamine synthetase (P0A040), ABC transporter, and Penicillin-binding proteins, ribosomal proteins, etc. It is seen that some of these proteins have been targeted in several other pathogenic bacteria to overcome survivability and drug resistance (Giordano et al. 2018; Prosser and de Carvalho 2013; Zhang et al. 2007; Liu et al. 2006; Kumar et al. 2018; Rehberg et al. 2019; Levy et al. 2008; He et al. 2020; Cui et al. 2019). So, targeting these essential non-host proteins in MRSA USA300 may pave the way to discovering new potential antibacterial therapeutics that can compromise the survivability of the drug-resistant *S. aureus*.

The clusters of peptidoglycan biosynthesis render a brief idea about the proteins responsible for antibiotic resistance. Peptidoglycan is the major heteropolymer of the bacterial cell wall that consists of alternate units of *N*-acetylglucosamine (GlcNAc) and *N*-acetylmuramoyl-peptides (MurNAc-peptide), thereby plays an essential role to protect the bacteria, maintaining characteristic cell shape and many more. Biosynthesis of cell-wall peptidoglycan starts with the formation of UDP-GlcNAc from fructose-6-phosphate, followed by the formation of UDP-MurNAc-pentapeptide from UDP-GlcNAc. In this study, Penicillin-binding protein Pbp2 and PbpA are identified interacting with femXAB family protein, mur-family proteins, Ddl and MraY etc. These bacterial essential proteins are always considered potential therapeutic targets for their cellular importance. MRSA strains have acquired a non-native penicillin-binding protein (PBP2a) which cross-links the peptidoglycan when the native staphylococcal PBPs are occupied by β -lactam antibiotics (Srisuknimit et al. 2017). Although the activity of *mecA* gene-encoded Pbp2a origins β -lactam resistance, recent observation shows that resistance can also be mediated by penicillin-binding protein 4 (PBP4) (Alexander et al. 2018). Thereby all the PBPs can be considered as potential targets against MRSA. The femA protein (P0A0A5) is essential for expressing high-level methicillin resistance in *S. aureus* (Maidhof et al. 1991; Fri et al. 2020). Three proteins of the femXAB family, FemX, FemA and FemB, catalyzes sequential addition of glycine residues from glycyl-t-RNAs to the muropeptid, thereby developing the methicillin-resistance (Berger-Bächli and Tschierske 1998;

Berger-Bächli 1999). The absence of functional femXAB proteins lead to improper cell-wall synthesis and increased susceptibility to β -lactam antibiotics (Rohrer et al. 1999; Kopp et al. 1996; Henze et al. 1993). MraY is a bacterial inner membrane protein essential for cell wall synthesis and targeted in antibiotic research studies (Hering et al. 2018). Recently, mur-family proteins are chosen as the prioritized drug targets from *Acinetobacter baumannii* (Amera et al. 2020). Methicillin resistance is a complex phenomenon and involves all the aforementioned proteins. It is seen that bacterial cell wall synthesis proteins directly or indirectly interacting with penicillin-binding proteins have a significant role in maintaining the cell-wall integrity and antibiotics resistance. So, targeting cell-wall synthesis proteins will give insights into bacterial antimicrobial research.

In this study, staphylococcal FemA (factors essential for methicillin-resistance A) protein accounts for structure-based virtual screening involving the drug repurposing approach due to its immense value in peptidoglycan biosynthesis as discussed earlier. The presence of FemA protein in other *S. aureus* pathogenic variants is checked using the default BLASTp search function of the DEG database. The search result shows that other than USA300_TCH1516, FemA also exists as an essential protein in MW2, MSSA476 and NCTC 8325 strains of *Staphylococcus aureus*. FemA crystal structure lacks several residues in its IB domain, the only active site. This may be due to the binding of the disaccharide hexapeptide lipid substrate (Benson et al. 2002). Thereby the active site is fixed using the modelling approach. Repurposing of drugs is a strategy for identifying new uses of approved or investigational old drugs. This strategy is advantageous due to the low risk of failure, reduced time frame for drug development and cost-effectiveness (Pushpakom et al. 2019). The drug repurposing approach successfully provides drugs for the treatment of AIDS, erectile dysfunction, rheumatoid arthritis, breast cancer, colorectal cancer and many more (Clouser et al. 2010; Ghofrani et al. 2006; Edwards et al. 2004; Sporn et al. 2004; Kune et al. 1988). Several reports tell about the success story of drug repurposing strategy. Recently, repurposing drugs that have been identified through in silico studies, are being used in the treatment of various diseases such as the ZIKA virus (Santos et al. 2020), SARS-CoV-2 (Zhang et al. 2020), malaria (Diallo et al. 2021) etc. These studies show that drug molecules are docked using AutoDock software and further experimentally checked with in vitro studies. AutoDock is an improved tool to provide accurate binding mode predictions (Trott and Olson 2009). In this study, docking analysis shows that identified FDA-approved drugs interact with the FemA protein with binding energies ranging between -7 and -11 kcal/mol. Irinotecan shows the highest binding affinity (-11.58 kcal/mol) towards staphylococcal femA with the K_i value of 3.23 nM, engaging the highest

number of hydrophobic interactions and four H-bonds. And Antrafenine holds the lowest binding energy (-7.36 kcal/mol) with the K_i value of 4050 nM, where only two H-bonds are present with less hydrophobic interactions. In general, hydrogen bonding increases the affinity of drugs towards their target. Besides, An increase in the number of hydrophobic atoms in the active core of the drug-protein interface increases the biological activity of the drug molecule (Patil et al. 2010). This defines the critical role of hydrophobic interactions in drug designing and development. Recent studies report that hydrogen bonds and hydrophobic interactions together play an important role in drug–target interactions with an approach to drug-repurposing (Choudhary et al. 2020; Chowdhury et al. 2020). Dexamethasone, Irinotecan, and Conivaptan are the drugs that show four hydrogen bonds each, though all drug molecules possess hydrogen bond interactions. Irinotecan, Midostaurin and Dihydroergotectan display the maximum number of hydrophobic interactions in the docked structure. In this study, molecular docking analysis reveals that the combinations of hydrogen bonds and hydrophobic interactions are the acting forces in drug–protein interaction; a significantly higher number of hydrophobic interactions are present over there. Interestingly, all hydrophobic residues are part of domain 1B, the catalytic site of FemA protein. Developing new drugs demands time and money thereby, this is always a challenge for the global pharmaceutical industry. So, there is an urgent demand to think differently to lower the investment and time to deliver a new drug to society, and this drug repurposing strategy has it all.

Conclusion

In this study, some novel therapeutic targets for *S. aureus* USA300 have been identified using in silico approach. These target proteins play a pivotal role in bacterial survival, infection establishment and pathogenesis. Cell-wall synthesis components are used to maintain structural integrity along with antibiotics resistance. Seven membrane proteins with prodigious immunogenic potential were screened as vaccine candidates. These prioritized targets include cell division proteins (Q2FZ91, Q2FZ95), penicillin-binding proteins (Q2FZ94, Q2FY10) of bacterial cell wall, pentose phosphate pathway component phosphoglucomutase (Q2FE11) and glycerolipid metabolism pathway component lipoteichoic acid synthase (Q2FIS2). A total of 53 potential drug targets are identified, which have shown similarity with the drug targets available in the DrugBank database. Altogether, 198 bacterial essential non-homologous proteins are identified that could be subjected to therapeutics development to be used to combat *S. aureus* mediated bacteremia. All the peptidoglycan biosynthesis enzymes are essential and specific,

therefore provide attractive potential targets for discovering and developing new antibacterials. Due to its biological importance, staphylococcal FemA has been considered an important therapeutic target. The structure-based virtual screening reveals ten potential repurposing drugs to target FemA. Predicted drugs require experimental validation that would lead to the development of new antimicrobial agents in this drug-resistance world.

Supplementary Information The online version contains supplementary material available at <https://doi.org/10.1007/s10989-021-10287-9>.

Acknowledgements Shakilur acknowledges the Indian Institute of Technology Kharagpur (IIT KGP) for individual fellowship. Mr Bharat Manna, School of Energy Science and Engineering, IIT KGP, is acknowledged for suggestions in structure-based virtual screening. Shakilur also wishes to acknowledge Mr Joydeep Baral and Ms Rituparna Saha, Department of Biotechnology, IIT KGP, for their critical review.

Author Contributions SR designed and carried out the experiments, formal analysis and wrote the draft manuscript. AKD conceptualized, supervised the study and checked the manuscript. All authors have read and agreed to the published version of the manuscript.

Funding This research did not receive any specific grant from funding agencies in the public, commercial, or not-for-profit sectors.

Declarations

Conflict of interest The authors declare no conflict of interest.

References

- Ain ul Q, Ahmad S, Azam SS (2018) Subtractive proteomics and immunoinformatics revealed novel B-cell derived T-cell epitopes against *Yersinia enterocolitica*: an etiological agent of Yersiniosis. *MicrOb Pathog* 125:336–348. <https://doi.org/10.1016/j.micpath.2018.09.042>
- Alexander JAN, Chatterjee SS, Hamilton SM, Eltis LD, Chambers HF, Strynadka NCJ (2018) Structural and kinetic analyses of penicillin-binding protein 4 (PBP4)-mediated antibiotic resistance in *Staphylococcus aureus*. *J Biol Chem* 293:19854–19865. <https://doi.org/10.1074/jbc.RA118.004952>
- Alvarez C, Barrientes O, Leal A, Contreras G, Barrero L, Rincon S, Diaz L, Vanegas N, Arias C (2006) Community-associated methicillin-resistant *Staphylococcus aureus*, Colombia. *Emerg Infect Dis* 12:2000–2001. <https://doi.org/10.3201/eid1212.060814>
- Amera GM, Khan RJ, Jha RK, Pathak A, Muthukumaran J, Singh AK (2020) Prioritization of Mur family drug targets against *A. baumannii* and identification of their homologous proteins through molecular phylogeny, primary sequence, and structural analysis. *J Genet Eng Biotechnol* 18:33. <https://doi.org/10.1186/s43141-020-00048-4>
- Bateman A (2019) UniProt: a worldwide hub of protein knowledge. *Nucleic Acids Res* 47:D506–D515. <https://doi.org/10.1093/nar/gky1049>
- Benkert P, Biasini M, Schwede T (2011) Toward the estimation of the absolute quality of individual protein structure models.

- Bioinformatics 27:343–350. <https://doi.org/10.1093/bioinformatics/btq662>
- Benson TE, Prince DB, Mutchler VT, Curry KA, Ho AM, Sarver RW, Hagadorn JC, Choi GH, Garlick RL (2002) X-ray crystal structure of *Staphylococcus aureus* FemA. *Structure* 10:1107–1115. [https://doi.org/10.1016/S0969-2126\(02\)00807-9](https://doi.org/10.1016/S0969-2126(02)00807-9)
- Berger-Bächli B (1999) Genetic basis of methicillin resistance in *Staphylococcus aureus*. *Cell Mol Life Sci* 56:764–770. <https://doi.org/10.1007/s000180050023>
- Berger-Bächli B, Tschierske M (1998) Role of fem factors in methicillin resistance. *Drug Resist Updat* 1:325–335. [https://doi.org/10.1016/S1368-7646\(98\)80048-4](https://doi.org/10.1016/S1368-7646(98)80048-4)
- Berry H, Coquelin JP, Gordon A, Seymour D (1983) Antrafenine, naproxen and placebo in osteoarthritis: a comparative study. *Br J Rheumatol* 22:89–94. <https://doi.org/10.1093/rheumatology/22.2.89>
- Bertelli C, Laird MR, Williams KP, Lau BY, Hoad G, Winsor GL, Brinkman FSL (2017) IslandViewer 4: expanded prediction of genomic islands for larger-scale datasets. *Nucleic Acids Res* 45:W30–W35. <https://doi.org/10.1093/nar/gkx343>
- Boratyn GM, Schäffer AA, Agarwala R, Altschul SF, Lipman DJ, Madden TL (2012) Domain enhanced lookup time accelerated BLAST. *Biol Direct* 7:12. <https://doi.org/10.1186/1745-6150-7-12>
- Buchanan JT, Stannard JA, Lauth X, Ostland VE, Powell HC, Westerman ME, Nizet V (2005) *Streptococcus iniae* phosphoglucosyltransferase is a virulence factor and a target for vaccine development. *Infect Immun* 73:6935–6944. <https://doi.org/10.1128/IAI.73.10.6935-6944.2005>
- Cadieux B, Vijayakumaran V, Bernards MA, McGavin MJ, Heinrichs DE (2014) Role of lipase from community-associated methicillin-resistant *Staphylococcus aureus* strain USA300 in hydrolyzing triglycerides into growth-inhibitory free fatty acids. *J Bacteriol* 196:4044–4056. <https://doi.org/10.1128/JB.02044-14>
- Caragea C, Caragea D, Silvescu A, Honavar V (2010) Semi-supervised prediction of protein subcellular localization using abstraction augmented Markov models. *BMC Bioinform* 11:S6. <https://doi.org/10.1186/1471-2105-11-S8-S6>
- Carleton HA, Diep BA, Charlebois ED, Sensabaugh GF, Perdreaux-Remington F (2004) Community-adapted methicillin-resistant *Staphylococcus aureus* (MRSA): population dynamics of an expanding community reservoir of MRSA. *J Infect Dis* 190:1730–1738. <https://doi.org/10.1086/425019>
- Chopra I, Roberts M (2001) Tetracycline antibiotics: mode of action, applications, molecular biology, and epidemiology of bacterial resistance. *Microbiol Mol Biol Rev* 65:232–260. <https://doi.org/10.1128/MMBR.65.2.232-260.2001>
- Choudhary S, Malik YS, Tomar S (2020) Identification of SARS-CoV-2 cell entry inhibitors by drug repurposing using in silico structure-based virtual screening approach. *Front Immunol* 11:1664. <https://doi.org/10.3389/fimmu.2020.01664>
- Chowdhury KH, Chowdhury MR, Mahmud S, Tareq AM, Hanif NB, Banu N, Reza ASMA, Bin ET, Simal-Gandara J (2020) Drug repurposing approach against novel coronavirus disease (COVID-19) through virtual screening targeting SARS-CoV-2 main protease. *Biology (basel)* 10:2. <https://doi.org/10.3390/biology10010002>
- Chua KYL, Monk IR, Lin Y-H, Seemann T, Tuck KL, Porter JL, Stepnell J, Coombs GW, Davies JK, Stinear TP, Howden BP (2014) Hyperexpression of α -hemolysin explains enhanced virulence of sequence type 93 community-associated methicillin-resistant *Staphylococcus aureus*. *BMC Microbiol* 14:31. <https://doi.org/10.1186/1471-2180-14-31>
- Clouser CL, Patterson SE, Mansky LM (2010) Exploiting drug repositioning for discovery of a novel HIV combination therapy. *J Virol* 84:9301–9309. <https://doi.org/10.1128/JVI.01006-10>
- Coe KA, Lee W, Stone MC, Komazin-Meredith G, Meredith TC, Grad YH, Walker S (2019) Multi-strain Tn-Seq reveals common daptomycin resistance determinants in *Staphylococcus aureus*. *PLOS Pathog* 15:e1007862. <https://doi.org/10.1371/journal.ppat.1007862>
- Cui W-Q, Qu Q-W, Wang J-P, Bai J-W, Bello-Onaghise G, Li Y-A, Zhou Y-H, Chen X-R, Liu X, Zheng S-D, Xing X-X, Eliphaz N, Li Y-H (2019) Discovery of potential anti-infective therapy targeting glutamine synthetase in *Staphylococcus xylosum*. *Front Chem* 7:381. <https://doi.org/10.3389/fchem.2019.00381>
- Diallo BN, Swart T, Hoppe HC, Tasthan Bishop Ö, Lobb K (2021) Potential repurposing of four FDA approved compounds with antiplasmodial activity identified through proteome scale computational drug discovery and in vitro assay. *Sci Rep*. <https://doi.org/10.1038/s41598-020-80722-2>
- Diekema DJ, Pfaller MA, Schmitz FJ, Smayevsky J, Bell J, Jones RN, Beach M (2001) Survey of infections due to *Staphylococcus* species: frequency of occurrence and antimicrobial susceptibility of isolates collected in the United States, Canada, Latin America, Europe, and the Western Pacific Region for the SENTRY antimicrobial surveillance program. *Clin Infect Dis* 32:S114–S132. <https://doi.org/10.1086/320184>
- Diekema DJ, Richter SS, Heilmann KP, Dohrn CL, Riahi F, Tendolkar S, McDanel JS, Doern KV (2014) Continued emergence of USA300 methicillin-resistant *Staphylococcus aureus* in the United States: results from a nationwide surveillance study. *Infect Control Hosp Epidemiol* 35:285–292. <https://doi.org/10.1086/675283>
- Doytchinova IA, Flower DR (2007) VaxiJen: a server for prediction of protective antigens, tumour antigens and subunit vaccines. *BMC Bioinformatics* 8:4. <https://doi.org/10.1186/1471-2105-8-4>
- Edwards JCW, Szczepański L, Szechiński J, Filipowicz-Sosnowska A, Emery P, Close DR, Stevens RM, Shaw T (2004) Efficacy of B-cell-targeted therapy with rituximab in patients with rheumatoid arthritis. *N Engl J Med* 350:2572–2581. <https://doi.org/10.1056/NEJMoa032534>
- Ehsan N, Ahmad S, Azam SS, Rungrotmongkol T, Uddin R (2018) Proteome-wide identification of epitope-based vaccine candidates against multi-drug resistant *Proteus mirabilis*. *Biologicals* 55:27–37. <https://doi.org/10.1016/j.biologicals.2018.07.004>
- Fischer T, Stone RM, DeAngelo DJ, Galinsky I, Estey E, Lanza C, Fox E, Ehninger G, Feldman EJ, Schiller GJ, Klimek VM, Nimer SD, Gilliland DG, Dutreix C, Huntsman-Labed A, Virkus J, Giles FJ (2010) Phase IIB trial of oral midostaurin (PKC412), the FMS-like tyrosine kinase 3 receptor (FLT3) and multi-targeted kinase inhibitor, in patients with acute myeloid leukemia and high-risk myelodysplastic syndrome with either wild-type or mutated FLT3. *J Clin Oncol* 28:4339–4345. <https://doi.org/10.1200/JCO.2010.28.9678>
- Fri J, Njom HA, Ateba CN, Ndip RN (2020) Antibiotic resistance and virulence gene characteristics of methicillin-resistant *Staphylococcus aureus* (MRSA) isolated from healthy edible marine fish. *Int J Microbiol* 2020:1–9. <https://doi.org/10.1155/2020/9803903>
- Fujita K (2015) Irinotecan, a key chemotherapeutic drug for metastatic colorectal cancer. *World J Gastroenterol* 21:12234. <https://doi.org/10.3748/wjg.v21.i43.12234>
- Ghali J (2009) Conivaptan and its role in the treatment of hyponatremia. *Drug Des Devel Ther* 3:253–268. <https://doi.org/10.2147/DDDT.S4505>
- Ghofrani HA, Osterloh IH, Grimminger F (2006) Sildenafil: from angina to erectile dysfunction to pulmonary hypertension and beyond. *Nat Rev Drug Discov* 5:689–702. <https://doi.org/10.1038/nrd2030>

- Giordano N, Hastie JL, Smith AD, Foss ED, Gutierrez-Munoz DF, Carlson PE (2018) Cysteine desulfurase IscS2 plays a role in oxygen resistance in *Clostridium difficile*. *Infect Immun*. <https://doi.org/10.1128/IAI.00326-18>
- Giulieri SG, Tong SYC, Williamson DA (2020) Using genomics to understand methicillin- and vancomycin-resistant *Staphylococcus aureus* infections. *Microb Genomics* 6:e000324. <https://doi.org/10.1099/mgen.0.000324>
- Goodsell DS, Zardecki C, Di Costanzo L, Duarte JM, Hudson BP, Persikova I, Segura J, Shao C, Voigt M, Westbrook JD, Young JY, Burley SK (2020) RCSB Protein Data Bank: enabling biomedical research and drug discovery. *Protein Sci* 29:52–65. <https://doi.org/10.1002/pro.3730>
- Guex N, Peitsch MC, Schwede T (2009) Automated comparative protein structure modeling with SWISS-MODEL and Swiss-Pdb-Viewer: a historical perspective. *Electrophoresis* 30:S162–S173. <https://doi.org/10.1002/elps.200900140>
- Hajduk PJ, Huth JR, Tse C (2005) Predicting protein druggability. *Drug Discovery Today*. [https://doi.org/10.1016/S1359-6446\(05\)03624-X](https://doi.org/10.1016/S1359-6446(05)03624-X)
- He J, Qiao W, An Q, Yang T, Luo Y (2020) Dihydrofolate reductase inhibitors for use as antimicrobial agents. *Eur J Med Chem* 195:112268. <https://doi.org/10.1016/j.ejmech.2020.112268>
- Henze U, Sidow T, Wecke J, Labischinski H, Berger-Bächi B (1993) Influence of femB on methicillin resistance and peptidoglycan metabolism in *Staphylococcus aureus*. *J Bacteriol* 175:1612–1620. <https://doi.org/10.1128/JB.175.6.1612-1620.1993>
- Hering J, Dunevall E, Ek M, Brändén G (2018) Structural basis for selective inhibition of antibacterial target MraY, a membrane-bound enzyme involved in peptidoglycan synthesis. *Drug Discov Today* 23:1426–1435. <https://doi.org/10.1016/j.drudis.2018.05.020>
- Hizbullah NZ, Afridi SG, Shah M, Shams S, Khan A (2018) Reverse vaccinology and subtractive genomics-based putative vaccine targets identification for *Burkholderia pseudomallei* Bp1651. *Microb Pathog* 125:219–229. <https://doi.org/10.1016/j.micpath.2018.09.033>
- Ibberson CB, Jones CL, Singh S, Wise MC, Hart ME, Zurawski DV, Horswill AR (2014) *Staphylococcus aureus* hyaluronidase is a CodY-regulated virulence factor. *Infect Immun* 82:4253–4264. <https://doi.org/10.1128/IAI.01710-14>
- Ikeuchi K, Adachi E, Sasaki T, Suzuki M, Lim LA, Saito M, Koga M, Tsutsumi T, Kido Y, Uehara Y, Yotsuyanagi H (2021) An outbreak of USA300 methicillin-resistant *Staphylococcus aureus* among people with HIV in Japan. *J Infect Dis* 223(4):610–620. <https://doi.org/10.1093/infdis/jiaa651>
- Ilinskaya AN, Dobrovolskaia MA (2016) Understanding the immunogenicity and antigenicity of nanomaterials: past, present and future. *Toxicol Appl Pharmacol* 299:70–77. <https://doi.org/10.1016/j.taap.2016.01.005>
- Ito T, Katayama Y, Hiramatsu K (1999) Cloning and nucleotide sequence determination of the entire mec DNA of pre-methicillin-resistant *Staphylococcus aureus* N315. *Antimicrob Agents Chemother* 43:1449–1458. <https://doi.org/10.1128/AAC.43.6.1449>
- Ito T, Katayama Y, Asada K, Mori N, Tsutsumimoto K, Tiensasitorn C, Hiramatsu K (2001) Structural comparison of three types of Staphylococcal Cassette Chromosome mec integrated in the chromosome in methicillin-resistant *Staphylococcus aureus*. *Antimicrob Agents Chemother* 45:1323–1336. <https://doi.org/10.1128/AAC.45.5.1323-1336.2001>
- Jadhav A, Ezhilarasan V, Prakash Sharma O, Pan A (2013) Clostridium-DTDB: s comprehensive database for potential drug targets of *Clostridium difficile*. *Comput Biol Med* 43:362–367. <https://doi.org/10.1016/j.combiomed.2013.01.009>
- Jenkins TC, McCollister BD, Sharma R, McFann KK, Madinger NE, Barron M, Bessesen M, Price CS, Burman WJ (2009) Epidemiology of healthcare-associated bloodstream infection caused by USA300 strains of methicillin-resistant *Staphylococcus aureus* in 3 affiliated hospitals. *Infect Control Hosp Epidemiol* 30:233–241. <https://doi.org/10.1086/595963>
- Jespersen MC, Peters B, Nielsen M, Marcatili P (2017) BepiPred-2.0: improving sequence-based B-cell epitope prediction using conformational epitopes. *Nucleic Acids Res* 45:W24–W29. <https://doi.org/10.1093/nar/gkx346>
- Jespersen MC, Mahajan S, Peters B, Nielsen M, Marcatili P (2019) Antibody specific B-cell epitope predictions: leveraging information from antibody-antigen protein complexes. *Front Immunol* 10:298. <https://doi.org/10.3389/fimmu.2019.00298>
- Johnson M, Zaretskaya I, Raytselis Y, Merezhuk Y, McGinnis S, Madden TL (2008) NCBI BLAST: a better web interface. *Nucleic Acids Res*. <https://doi.org/10.1093/nar/gkn201>
- Kanehisa M, Furumichi M, Sato Y, Ishiguro-Watanabe M, Tanabe M (2021) KEGG: integrating viruses and cellular organisms. *Nucleic Acids Res* 49:D545–D551. <https://doi.org/10.1093/nar/gkaa970>
- Kaya H, Hasman H, Larsen J, Stegger M, Johannesen TB, Allesøe RL, Lemvig CK, Aarestrup FM, Lund O, Larsen AR (2018) SCCmecFinder, a web-based tool for typing of Staphylococcal Cassette Chromosome mec in *Staphylococcus aureus* using whole-genome sequence data. *mSphere*. 3:e00612-17. <https://doi.org/10.1128/mSphere.00612-17>
- Keam SJ, Plosker GL (2007) Rupatadine. *Drugs* 67:457–474. <https://doi.org/10.2165/00003495-200767030-00008>
- Kelley LA, Mezulis S, Yates CM, Wass MN, Sternberg MJE (2015) The Phyre2 web portal for protein modeling, prediction and analysis. *Nat Protoc* 10:845–858. <https://doi.org/10.1038/nprot.2015.053>
- Kim DE, Chivian D, Baker D (2004) Protein structure prediction and analysis using the Robetta server. *Nucleic Acids Res* 32:W526–W531. <https://doi.org/10.1093/nar/gkh468>
- Kluytmans J, van Belkum A, Verbrugh H (1997) Nasal carriage of *Staphylococcus aureus*: epidemiology, underlying mechanisms, and associated risks. *Clin Microbiol Rev* 10:505–520. <https://doi.org/10.1128/CMR.10.3.505-520.1997>
- Ko Y-P, Kuipers A, Freitag CM, Jongerius I, Medina E, van Rooijen WJ, Spaan AN, van Kessel KPM, Höök M, Rooijackers SHM (2013) Phagocytosis escape by a *Staphylococcus aureus* protein that connects complement and coagulation proteins at the bacterial surface. *PLoS Pathog* 9:e1003816. <https://doi.org/10.1371/journal.ppat.1003816>
- Kopp U, Roos M, Wecke J, Labischinski H (1996) Staphylococcal peptidoglycan interpeptide bridge biosynthesis: a novel antistaphylococcal target? *Microb Drug Resist* 2:29–41. <https://doi.org/10.1089/mdr.1996.2.29>
- Kumar V, Sharma A, Pratap S, Kumar P (2018) Biophysical and in silico interaction studies of aporphine alkaloids with Malonyl-CoA: ACP transacylase (FabD) from drug resistant *Moraxella catarrhalis*. *Biochimie* 149:18–33. <https://doi.org/10.1016/j.biochi.2018.03.012>
- Kune GA, Kune S, Watson LF (1988) Colorectal cancer risk, chronic illnesses, operations, and medications: case control results from the Melbourne Colorectal Cancer Study. *Cancer Res* 48:4399–4404
- Laabei M, Uhlemann A-C, Lowy FD, Austin ED, Yokoyama M, Ouadi K, Feil E, Thorpe HA, Williams B, Perkins M, Peacock SJ, Clarke SR, Dordel J, Holden M, Votintseva AA, Bowden R, Crook DW, Young BC, Wilson DJ, Recker M et al (2015) Evolutionary trade-offs underlie the multi-faceted virulence of

- Staphylococcus aureus*. PLoS Biol 13:e1002229. <https://doi.org/10.1371/journal.pbio.1002229>
- Laskowski RA, Swindells MB (2011) LigPlot+: multiple ligand–protein interaction diagrams for drug discovery. J Chem Inf Model 51:2778–2786. <https://doi.org/10.1021/ci200227u>
- Laskowski RA, MacArthur MW, Moss DS, Thornton JM (1993) PROCHECK: a program to check the stereochemical quality of protein structures. J Appl Crystallogr 26:283–291. <https://doi.org/10.1107/S0021889892009944>
- Laupland KB, Ross T, Gregson DB (2008) *Staphylococcus aureus* bloodstream infections: risk factors, outcomes, and the influence of methicillin resistance in Calgary, Canada, 2000–2006. J Infect Dis 198:336–343. <https://doi.org/10.1086/589717>
- Levy C, Minnis D, Derrick JP (2008) Dihydropteroate synthase from *Streptococcus pneumoniae*: structure, ligand recognition and mechanism of sulfonamide resistance. Biochem J 412:379–388. <https://doi.org/10.1042/BJ20071598>
- Lewin GR, Stacy A, Michie KL, Lamont RJ, Whiteley M (2019) Large-scale identification of pathogen essential genes during coinfection with sympatric and allopatric microbes. Proc Natl Acad Sci 116:19685–19694. <https://doi.org/10.1073/pnas.1907619116>
- Li W, Joshi M, Singhanian S, Ramsey K, Murthy A (2014) Peptide vaccine: progress and challenges. Vaccines 2:515–536. <https://doi.org/10.3390/vaccines2030515>
- Lina G, Bohach GA, Nair SP, Hiramatsu K, Jouvin-Marche E, Mariuzza R (2004) Standard nomenclature for the superantigens expressed by *Staphylococcus*. J Infect Dis 189:2334–2336. <https://doi.org/10.1086/420852>
- Lipton RB, Croop R, Stock EG, Stock DA, Morris BA, Frost M, Dubowchik GM, Conway CM, Coric V, Goadsby PJ (2019) Rimegepant, an oral calcitonin gene-related peptide receptor antagonist, for migraine. N Engl J Med 381:142–149. <https://doi.org/10.1056/NEJMoa1811090>
- Liu W, Han C, Hu L, Chen K, Shen X, Jiang H (2006) Characterization and inhibitor discovery of one novel malonyl-CoA: acyl carrier protein transacylase (MCAT) from *Helicobacter pylori*. FEBS Lett 580:697–702. <https://doi.org/10.1016/j.febslet.2005.12.085>
- Liu B, Zheng D, Jin Q, Chen L, Yang J (2019) VFDB 2019: a comparative pathogenomic platform with an interactive web interface. Nucleic Acids Res 47:D687–D692. <https://doi.org/10.1093/nar/gky1080>
- Luo H, Lin Y, Gao F, Zhang C-T, Zhang R (2014) DEG 10, an update of the database of essential genes that includes both protein-coding genes and noncoding genomic elements: table 1. Nucleic Acids Res 42:D574–D580. <https://doi.org/10.1093/nar/gkt1131>
- Maidhof H, Reinicke B, Blümel P, Berger-Bächi B, Labischinski H (1991) femA, which encodes a factor essential for expression of methicillin resistance, affects glycine content of peptidoglycan in methicillin-resistant and methicillin-susceptible *Staphylococcus aureus* strains. J Bacteriol 173:3507–3513. <https://doi.org/10.1128/JB.173.11.3507-3513.1991>
- Matossian M, Vangelder C, Papagerakis P, Zheng L, Wolf GT, Papagerakis S (2014) In silico modeling of the molecular interactions of antacid medication with the endothelium: novel therapeutic implications in head and neck carcinomas. Int J Immunopathol Pharmacol 27(4):573–583. <https://doi.org/10.1177/039463201402700413>
- Moller S, Croning MDR, Apweiler R (2001) Evaluation of methods for the prediction of membrane spanning regions. Bioinformatics 17:646–653. <https://doi.org/10.1093/bioinformatics/17.7.646>
- Monteiro JM, Covas G, Rausch D, Filipe SR, Schneider T, Sahl H-G, Pinho MG (2019) The pentaglycine bridges of *Staphylococcus aureus* peptidoglycan are essential for cell integrity. Sci Rep 9:5010. <https://doi.org/10.1038/s41598-019-41461-1>
- Moran GJ, Krishnadasan A, Gorwitz RJ, Fosheim GE, McDougal LK, Carey RB, Talan DA (2006) Methicillin-resistant *S. aureus* infections among patients in the emergency department. N Engl J Med 355:666–674. <https://doi.org/10.1056/NEJMoa055356>
- Morris GM, Huey R, Olson AJ (2008) Using AutoDock for ligand–receptor docking. Curr Protoc Bioinform 24:8.14.1–8.14.40. <https://doi.org/10.1002/0471250953.bi0814s24>
- Morris GM, Huey R, Lindstrom W, Sanner MF, Belew RK, Goodsell DS, Olson AJ (2009) AutoDock4 and AutoDockTools4: automated docking with selective receptor flexibility. J Comput Chem 30:2785–2791. <https://doi.org/10.1002/jcc.21256>
- Nikolaïdis I, Favini-Stabile S, Dessen A (2014) Resistance to antibiotics targeted to the bacterial cell wall. Protein Sci Publ Protein Soc 23(3):243–259. <https://doi.org/10.1002/pro.2414>
- O’Boyle NM, Banck M, James CA, Morley C, Vandermeersch T, Hutchison GR (2011) Open label: an open chemical toolbox. J Cheminform 3:33. <https://doi.org/10.1186/1758-2946-3-33>
- O’Leary NA, Wright MW, Brister JR, Ciufu S, Haddad D, McVeigh R, Rajput B, Robbette B, Smith-White B, Ako-Adjei D, Astashyn A, Badredin A, Bao Y, Blinkova O, Brover V, Chetvernin V, Choi J, Cox E, Ermolaeva O, Farrell CM et al (2016) Reference sequence (RefSeq) database at NCBI: current status, taxonomic expansion, and functional annotation. Nucleic Acids Res 44:D733–D745. <https://doi.org/10.1093/nar/gkv1189>
- Otero LH, Rojas-Altuve A, Llarrull LI, Carrasco-Lopez C, Kumarasiri M, Lastochkin E, Fishovitz J, Dawley M, Heseck D, Lee M, Johnson JW, Fisher JF, Chang M, Mobashery S, Hermoso JA (2013) How allosteric control of *Staphylococcus aureus* penicillin binding protein 2a enables methicillin resistance and physiological function. Proc Natl Acad Sci 110:16808–16813. <https://doi.org/10.1073/pnas.1300118110>
- Patil R, Das S, Stanley A, Yadav L, Sudhakar A, Varma AK (2010) Optimized hydrophobic interactions and hydrogen bonding at the target–ligand interface leads the pathways of drug-designing. PLoS ONE 5:e12029. <https://doi.org/10.1371/journal.pone.0012029>
- Peacock SJ, de Silva I, Lowy FD (2001) What determines nasal carriage of *Staphylococcus aureus*? Trends Microbiol. [https://doi.org/10.1016/S0966-842X\(01\)02254-5](https://doi.org/10.1016/S0966-842X(01)02254-5)
- Pearson WR (1995) Comparison of methods for searching protein sequence databases. Protein Sci 4:1145–1160. <https://doi.org/10.1002/pro.5560040613>
- Pearson WR (1996) Effective protein sequence comparison. Methods in enzymology. Elsevier, Amsterdam, pp 227–258. [https://doi.org/10.1016/S0076-6879\(96\)66017-0](https://doi.org/10.1016/S0076-6879(96)66017-0)
- Pettersen EF, Goddard TD, Huang CC, Couch GS, Greenblatt DM, Meng EC, Ferrin TE (2004) UCSF Chimera—a visualization system for exploratory research and analysis. J Comput Chem 25:1605–1612. <https://doi.org/10.1002/jcc.20084>
- Planet PJ, LaRussa SJ, Dana A, Smith H, Xu A, Ryan C, Uhlemann A-C, Boundy S, Goldberg J, Narechania A, Kulkarni R, Ratner AJ, Geoghegan JA, Kolokotronis S-O, Prince A (2013) Emergence of the epidemic methicillin-resistant *Staphylococcus aureus* strain USA300 coincides with horizontal transfer of the arginine catabolic mobile element and speG-mediated adaptations for survival on skin. Mbio 4:e00889–e913. <https://doi.org/10.1128/mBio.00889-13>
- Prosser GA, de Carvalho LPS (2013) Metabolomics reveal D-alanine:D-alanine ligase as the target of D-cycloserine in *Mycobacterium tuberculosis*. ACS Med Chem Lett 4:1233–1237. <https://doi.org/10.1021/ml400349n>
- Pushpakom S, Iorio F, Eyers PA, Escott KJ, Hopper S, Wells A, Doig A, Guilliams T, Latimer J, McNamee C, Norris A, Sanseau P, Cavalla D, Pirmohamed M (2019) Drug repurposing: progress, challenges and recommendations. Nat Rev Drug Discov 18:41–58. <https://doi.org/10.1038/nrd.2018.168>
- Rajan V, Schoenfelder SMK, Ziebuhr W, Gopal S (2015) Genotyping of community-associated methicillin resistant *Staphylococcus*

- aureus* (CA-MRSA) in a tertiary care centre in Mysore, South India: ST2371-SCCmec IV emerges as the major clone. *Infect Genet Evol* 34:230–235. <https://doi.org/10.1016/j.meegid.2015.05.032>
- Rashid MI, Naz A, Ali A, Andleeb S (2017) Prediction of vaccine candidates against *Pseudomonas aeruginosa*: an integrated genomics and proteomics approach. *Genomics* 109:274–283. <https://doi.org/10.1016/j.ygeno.2017.05.001>
- Rehberg N, Omeje E, Ebada SS, van Geelen L, Liu Z, Surechatchayan P, Kassack MU, Ioerger TR, Proksch P, Kalscheuer R (2019) 3-O-methyl-alkylgallates inhibit fatty acid desaturation in *Mycobacterium tuberculosis*. *Antimicrob Agents Chemother* 63:e00136–e219. <https://doi.org/10.1128/AAC.00136-19>
- Rohrer S, Ehler K, Tschierske M, Labischinski H, Berger-Bachi B (1999) The essential *Staphylococcus aureus* gene *fmhB* is involved in the first step of peptidoglycan pentaglycine interpeptide formation. *Proc Natl Acad Sci* 96:9351–9356. <https://doi.org/10.1073/pnas.96.16.9351>
- Saha S, Raghava GPS (2006) Prediction of continuous B-cell epitopes in an antigen using recurrent neural network. *Proteins Struct Funct Bioinform* 65:40–48. <https://doi.org/10.1002/prot.21078>
- Sanchez-Trincado JL, Gomez-Perosanz M, Reche PA (2017) Fundamentals and methods for T- and B-cell epitope prediction. *J Immunol Res* 2017:1–14. <https://doi.org/10.1155/2017/2680160>
- Santos FRS, Nunes DAF, Lima WG, Davyt D, Santos LL, Taranto AG, Ferreira MSJ (2020) Identification of Zika virus NS2B-NS3 protease inhibitors by structure-based virtual screening and drug repurposing approaches. *J Chem Inform Model* 60(2):731. <https://doi.org/10.1021/acs.jcim.9b00933>
- Sarkar M, Maganti L, Ghoshal N, Dutta C (2012) In silico quest for putative drug targets in *Helicobacter pylori* HPAG1: molecular modeling of candidate enzymes from lipopolysaccharide biosynthesis pathway. *J Mol Model* 18:1855–1866. <https://doi.org/10.1007/s00894-011-1204-3>
- Schürks M (2009) Dihydroergotamine: role in the treatment of migraine. *Expert Opin Drug Metab Toxicol* 5:1141–1148. <https://doi.org/10.1517/17425250903164211>
- Shah M, Jaan S, Fatima B, Javed MS, Amjad A, Khan A, Afridi SG, Nishan U, Iqbal A, Nawaz H (2021) Delineating novel therapeutic drug and vaccine targets for *Staphylococcus cornubiensis* NWIT through computational analysis. *Int J Pept Res Ther* 27:181–195. <https://doi.org/10.1007/s10989-020-10076-w>
- Sibbald MJJB, Ziebandt AK, Engelmann S, Hecker M, de Jong A, Harmsen HJM, Raangs GC, Stokroos I, Arends JP, Dubois JYF, van Dijk JM (2006) Mapping the pathways to staphylococcal pathogenesis by comparative secretomics. *Microbiol Mol Biol Rev* 70:755–788. <https://doi.org/10.1128/MMBR.00008-06>
- Silver LL (2011) Challenges of antibacterial discovery. *Clin Microbiol Rev* 24:71–109. <https://doi.org/10.1128/CMR.00030-10>
- Simor AE, Gilbert NL, Gravel D, Mulvey MR, Bryce E, Loeb M, Matlow A, McGeer A, Louie L, Campbell J (2010) Methicillin-resistant *Staphylococcus aureus* colonization or infection in Canada: national surveillance and changing epidemiology, 1995–2007. *Infect Control Hosp Epidemiol* 31:348–356. <https://doi.org/10.1086/651313>
- Solanki V, Tiwari M, Tiwari V (2019) Prioritization of potential vaccine targets using comparative proteomics and designing of the chimeric multi-epitope vaccine against *Pseudomonas aeruginosa*. *Sci Rep* 9:5240. <https://doi.org/10.1038/s41598-019-41496-4>
- Sporn MB, Dowsett SA, Mershon J, Bryant HU (2004) Role of raloxifene in breast cancer prevention in postmenopausal women: clinical evidence and potential mechanisms of action. *Clin Ther* 26:830–840. [https://doi.org/10.1016/s0149-2918\(04\)90127-0](https://doi.org/10.1016/s0149-2918(04)90127-0)
- Srisuknimit V, Qiao Y, Schaefer K, Kahne D, Walker S (2017) Peptidoglycan cross-linking preferences of *Staphylococcus aureus* penicillin-binding proteins have implications for treating MRSA infections. *J Am Chem Soc* 139:9791–9794. <https://doi.org/10.1021/jacs.7b04881>
- Strauß L, Stegger M, Akpaka PE, Alabi A, Breurec S, Coombs G, Egyir B, Larsen AR, Laurent F, Monecke S, Peters G, Skov R, Strommenger B, Vandenesch F, Schaumburg F, Mellmann A (2017) Origin, evolution, and global transmission of community-acquired *Staphylococcus aureus* ST8. *Proc Natl Acad Sci USA* 114(49):E10596–E10604. <https://doi.org/10.1073/pnas.1702472114>
- Szklarczyk D, Gable AL, Lyon D, Junge A, Wyder S, Huerta-Cepas J, Simonovic M, Doncheva NT, Morris JH, Bork P, Jensen LJ, von Mering C (2019) STRING v11: protein–protein association networks with increased coverage, supporting functional discovery in genome-wide experimental datasets. *Nucleic Acids Res* 47:D607–D613. <https://doi.org/10.1093/nar/gky1131>
- Takadama S, Nakaminami H, Kaneko H, Noguchi N (2020) A novel community-acquired MRSA clone, USA300-LV/J, uniquely evolved in Japan. *J Antimicrob Chemother* 75:3131–3134. <https://doi.org/10.1093/jac/dkaa313>
- Talan DA, Krishnadasan A, Gorwitz RJ, Fosheim GE, Limbago B, Albrecht V, Moran GJ, EMERGEncy ID Net Study Group (2011) Comparison of *Staphylococcus aureus* from skin and soft-tissue infections in US emergency department patients, 2004 and 2008. *Clin Infect Dis* 53:144–149. <https://doi.org/10.1093/cid/cir308>
- Tfelt-Hansen P (2000) Ergotamine in the acute treatment of migraine: a review and European consensus. *Brain* 123:9–18. <https://doi.org/10.1093/brain/123.1.9>
- Trott O, Olson AJ (2009) AutoDock Vina: improving the speed and accuracy of docking with a new scoring function, efficient optimization, and multithreading. *J Comput Chem*. <https://doi.org/10.1002/jcc.21334>
- Vita R, Mahajan S, Overton JA, Dhanda SK, Martini S, Cantrell JR, Wheeler DK, Sette A, Peters B (2019) The Immune Epitope Database (IEDB): 2018 update. *Nucleic Acids Res* 47:D339–D343. <https://doi.org/10.1093/nar/gky1006>
- Vollmer W, Blanot D, de Pedro MA (2008) Peptidoglycan structure and architecture. *FEMS Microbiol Rev* 32(2):149. <https://doi.org/10.1111/j.1574-6976.2007.00094.x>
- Waterhouse A, Bertoni M, Bienert S, Studer G, Tauriello G, Gumienny R, Heer FT, de Beer TAP, Rempfer C, Bordoli L, Lepore R, Schwede T (2018) SWISS-MODEL: homology modelling of protein structures and complexes. *Nucleic Acids Res* 46:W296–W303. <https://doi.org/10.1093/nar/gky427>
- Weese JS, van Duijkeren E (2010) Methicillin-resistant *Staphylococcus aureus* and *Staphylococcus pseudintermedius* in veterinary medicine. *Vet Microbiol* 140:418–429. <https://doi.org/10.1016/j.vetmic.2009.01.039>
- Wiederstein M, Sippl MJ (2007) ProSA-web: interactive web service for the recognition of errors in three-dimensional structures of proteins. *Nucleic Acids Res* 35:W407–W410. <https://doi.org/10.1093/nar/gkm290>
- Wishart DS, Feunang YD, Guo AC, Lo EJ, Marcu A, Grant JR, Sajed T, Johnson D, Li C, Sayeeda Z, Assempour N, Iynkkaran I, Liu Y, Maciejewski A, Gale N, Wilson A, Chin L, Cummings R, Le D, Pon A, Knox C, Wilson M (2017) DrugBank 5.0: a major update to the DrugBank database for 2018. *Nucleic Acids Res*. <https://doi.org/10.1093/nar/gkx1037>
- Wu C, Kapoor A (2013) Dutasteride for the treatment of benign prostatic hyperplasia. *Expert Opin Pharmacother* 14:1399–1408. <https://doi.org/10.1517/14656566.2013.797965>
- Yu C-S, Chen Y-C, Lu C-H, Hwang J-K (2006) Prediction of protein subcellular localization. *Proteins* 64:643–651. <https://doi.org/10.1002/prot.21018>
- Yu NY, Wagner JR, Laird MR, Melli G, Rey S, Lo R, Dao P, Sahinalp SC, Ester M, Foster LJ, Brinkman FSL (2010) PSORTb

- 3.0: improved protein subcellular localization prediction with refined localization subcategories and predictive capabilities for all prokaryotes. *Bioinformatics* 26:1608–1615. <https://doi.org/10.1093/bioinformatics/btq249>
- Zaharieva N, Dimitrov I, Flower DR, Doytchinova I (2019) VaxiJen dataset of bacterial immunogens: an update. *Curr Comput Aided Drug Des* 15:398–400. <https://doi.org/10.2174/1573409915666190318121838>
- Zhang L, Liu W, Xiao J, Hu T, Chen J, Chen K, Jiang H, Shen X (2007) Malonyl-CoA: acyl carrier protein transacylase from *Helicobacter pylori*: crystal structure and its interaction with acyl carrier protein. *Protein Sci* 16:1184–1192. <https://doi.org/10.1110/ps.072757307>
- Zhang H, Yang Y, Li J, Wang M, Saravanan KM, Wei J, Tze-Yang Ng J, Hossain MT, Liu M, Zhang H, Ren X, Pan Y, Peng Y, Shi Y, Wan X, Liu Y, Wei Y (2020) A novel virtual screening procedure identifies Pralatrexate as inhibitor of SARS-CoV-2 RdRp and it reduces viral replication in vitro. *PLOS Comput Biol* 16(12):1–5. <https://doi.org/10.1371/journal.pcbi.1008489>

Publisher's Note Springer Nature remains neutral with regard to jurisdictional claims in published maps and institutional affiliations.